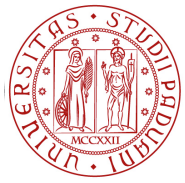

UNIVERSITÀ
DEGLI STUDI
DI PADOVA

Sede Amministrativa: Università degli Studi di Padova

Dipartimento di *Biomedicina Comparata e Alimentazione*- BCA

SCUOLA DI DOTTORATO DI RICERCA IN SCIENZE VETERINARIE

INDIRIZZO: UNICO

XXVIII CICLO

COMPUTED TOMOGRAPHIC EVALUATION OF CANINE PHARYNGEAL NEOPLASIA

Direttore della Scuola: Ch.mo Prof. Gianfranco Gabai

Supervisore: Ch.mo Prof. Alessandro Zotti

Dottorando : Dott. Gregorio Carozzi

SUMMARY:

Computed tomography (CT) is commonly used to investigate head tumours in dogs, and is a fundamental part of the diagnostic work-up, for diagnosis, staging and planning therapy in neoplastic disease. Nasal diseases, either neoplastic or non-neoplastic diseases, oral neoplasia, brain disease, thyroid or carotid body neoplasia have been extensively studied. However little information are available for lesions of the pharyngeal area.

In this thesis, cases of dogs affected by pharyngeal neoplasia have been collected from the database of three private referral veterinary clinics for diagnostic imaging. The purpose of this multicentric retrospective study was to analyse the CT findings in 25 dogs affected by pharyngeal neoplasia to identify features possibly differentiating the tumour type. Further aim was to analyse the distribution and pattern of presentation of regional lymphadenopathy (mandibular and medial retropharyngeal lymph nodes) to have particular features that might indicate nodal metastatic spread enabling more accurate patient staging.

In the **Chapter 1** the gross anatomy of the pharynx, its subdivision in nasal, oral and laryngeal part, the lymphatic drainage and the computed tomographic features and landmarks of these structures are described. The most important anatomical structures bounding the pharyngeal cavity and the most important structures surrounding the different pharyngeal parts have been identified and labelled, basing on available literature and anatomical images, and then matched on a sequence of computed tomographic images.

In the **Chapter 2** has been reported the most common pharyngeal neoplasia in the dog, in descending order malignant melanoma, squamous cell carcinoma, and fibrosarcoma. The epidemiologic, clinical and biologic behaviour of these cancers have some features overlapping with the human cancer. These features, along with the relative shortness of the life span of the dog,

and closely sharing of man's environment makes the dog an excellent animal model for comparative epidemiologic studies.

In the **Chapter 3** the tumour-nodal-metastasis (TNM) system provided by the World Health Organization for the staging of canine tumour is reported. Furthermore the imaging criteria, reported in human and veterinary literature assessed to evaluate the potential nodal involvement has been reviewed and compared.

In the **Chapter 4** are reported the Material and Methods regarding the inclusion criteria of the cases, the computed tomographic protocol adopted, the computed tomographic features considered, and the criteria of analysis, and the statistical procedures. The imaging features has been divided in qualitative features including location of lesions, shape, margins, relationship with adjacent structures and vessels, attenuation characteristics, pattern and grade of enhancement, changes in lymph nodes size, shape and enhancement and presence of potential distant metasasis; and quantitative features including the measure of volume, and pre and postcontrast attenuation expressed in Hounsfiled Units (HU). The effect of final diagnosis on each CT feature was statistically tested.

In the **Chapter 5** the caseload population and the results of the imaging and statistical analysis are described. The caseload included: 15 carcinomas, 5 sarcomas, 4 melanomas and 1 lymphoma. The oropharynx and laryngopharynx were more frequently involved. Lesions in the different groups were of similar size, irregular shape, ill-defined margins and moderate-to-marked heterogeneous contrast enhancement. Lysis of hyoid bones was recorded in two carcinomas and infiltration of the lingual artery in one case. Marked medial retropharyngeal lymphoadenomegaly was recorded in 11/14 carcinomas, in all sarcomas and in 2/4 melanomas. The single lymphoma case showed ill-

defined thickening of the oropharyngeal and laryngeal wall as well as both retropharyngeal and mandibular lymphadenomegaly. Lung metastases were found in 2/5 sarcomas and 2/4 melanomas.

In the **Chapter 6** the findings of this thesis are discussed. Findings indicate that computed tomography is precise and it has a good sensitivity in determining mass extension, lymph node involvement and distant metastatic spread. Nevertheless computed tomography specificity is low because most of the CT features were overlapping in the different groups of neoplasia, thus the biopsy is always required for a final diagnosis. However computed tomography is fundamental to assess nodal metastasis particularly in those lymph nodes not easily achievable during clinical examination. Furthermore the medial retropharyngeal lymph nodes are most frequently and severely involved than mandibular lymph nodes, and their analysis should be included in staging of pharyngeal neoplasia.

SOMMARIO:

L'esame tomografico computerizzato è comunemente usato per indagare le neoplasie a carico della regione della testa ed è parte integrante del percorso diagnostico dei pazienti oncologici, per la diagnosi, la stadiazione ed il *planning* terapeutico. Le patologie nasali sia neoplastiche che non neoplastiche, le neoplasie a carico del cavo orale, patologie cerebrali, i tumori tiroide e dei glomi carotidei sono state largamente studiate. Tuttavia poco o nulla è stato descritto in merito alle patologie che interessano la regione faringea.

In questa tesi sono stati raccolti i casi di cani con neoplasie del cavo faringeo, raccolte dal *database* di tre cliniche veterinarie di referenza per la diagnostica per immagini. Lo scopo di questo studio retrospettivo multicentrico è quello di analizzare le caratteristiche *imaging* di 25 cani che presentano neoplasie faringee per identificare le possibile caratteristiche che potrebbero differenziare i diversi tipi di tumore. Inoltre questo studio si propone di descrivere e analizzare la distribuzione e le caratteristiche *imaging* delle alterazioni patologiche dei linfonodi regionali (linfonodi mandibolari e retrofaringei mediali) allo scopo di individuare caratteristiche peculiari che potrebbero indicare una possibile disseminazione metastatica e quindi permettere una migliore stadiazione dei pazienti.

Nel **Capitolo 1** viene descritta la normale anatomia macroscopica della faringe, la relativa suddivisione nei tratti naso-, oro- e laringofaringei; il sistema linfatico e le caratteristiche tomografiche ed i punti di repere delle diverse strutture. Le principali strutture anatomiche sono state individuate Vengono riportate una sequenza d'immagini tomografiche in cui sono indicate le principali strutture anatomiche più importanti che delimitano la cavità.

Nel **Capitolo 2** sono state riportate le più comuni neoplasie faringee del cane. In ordine discendete troviamo il melanoma, il carcinoma squamoso cellulare ed il fibrosarcoma. Il comportamento biologico, alcuni aspetti clinici ed epidemiologici di questi tumori sono simili a quelli riportati in

medicina umana. Queste caratteristiche assieme alla relativa brevità della vita del cane ed al fatto che questa specie condivide strettamente lo stesso ambiente dell'uomo, ne fanno un eccellente modello animale per gli studi di epidemiologia comparata.

Nel **Capitolo 3** viene riportato il sistema TNM (Tumour-Nodal-Metastasis) approvato dalla World Health Organization per la stadiazione delle patologie neoplastiche nel cane. Inoltre sono stati riesaminati i criteri *imaging* utilizzati in medicina umana ed in medicina veterinaria per la valutazione delle alterazioni a carico dei linfonodi.

Nel **Capitolo 4** comprende la sezione dei Materiali e Metodi riguardanti i criteri di inclusione dei casi individuati, i protocolli di acquisizione delle immagini, le caratteristiche tomografiche considerate e i relativi criteri di analisi e le procedure di analisi statistica. Le caratteristiche *imaging* sono state suddivise in caratteristiche qualitative e quantitative. Le caratteristiche qualitative comprendono la localizzazione delle lesioni, la forma, i margini, i rapporti con le strutture circostanti e le strutture vascolari, le caratteristiche di attenuazione, il pattern ed il grado di *enhancement*, variazioni di dimensione, forma ed *enhancement* delle strutture linfonodali e la presenza di potenziali lesioni metastatiche a distanza. Le caratteristiche quantitative comprendono le misurazioni delle dimensioni e del volume delle lesioni e la loro attenuazione pre e postcontrasto espressa in Unità Hounsfield (HU). È stato testato l'effetto della diagnosi finale su ogni singola caratteristica analizzata.

Nel **Capitolo 5** vengono descritte la popolazione dei soggetti che rientravano nei criteri di inclusione, i risultati dell'analisi *imaging* e dell'analisi statistica. La casistica include: 15 carcinomi, 5 sarcomi, 4 melanomi e 1 linfoma. L'orofaringe e la laringofaringe sono state le regioni più coinvolte. Lesioni dei diversi gruppi presentavano dimensioni simili, forma irregolare, margini mal definiti, con enhancement eterogeneo che variava dal moderato al marcato. La lisi dell'oso ioide è

stata riscontrata in due carcinomi, mentre l'infiltrazione dell'arteria linguale è stata riportata in un solo caso. In 11/14 carcinomi, in tutti i sarcomi e in 2/4 melanomi è stata riscontrata una marcata linfadenomegalia retrofaringea mediale. Il singolo caso di linfoma si presentava come un irregolare e mal definito ispessimento della parete orofaringea e laringofaringea, associata a linfadenomegalia mandibolare e retrofaringea mediale bilaterale. Metastasi polmonari sono state individuate in 2/5 sarcomi e 2/4 melanomi.

Nel **Capitolo 6** vengono discussi e commentati i risultati dello studio. I risultati indicano che l'esame TC è preciso ed ha una buona sensibilità nell'individuare e determinarne l'estensione delle lesioni, indicare il coinvolgimento dei linfonodi regionali e la disseminazione metastatica regionale e a distanza. Ciononostante l'esame TC non si è rivelato essere altrettanto specifico poiché le lesioni presentano caratteristiche simili, pertanto l'esame istologico o citologico è sempre necessario per ottenere una diagnosi certa. Tuttavia l'esame tomografico è fondamentale per la valutazione di metastasi linfonodali, in particolare in quei linfonodi che non sono raggiungibili durante l'esame clinico. Inoltre, i linfonodi retrofaringei mediali sono stati più frequentemente e gravemente coinvolti rispetto ai linfonodi mandibolari e per questo dovrebbero essere inclusi nella stadiazione di neoplasie faringee.

CHAPTER 1

ANATOMY OF THE NORMAL PHARYNX

1.1 INTRODUCTION

The respiratory system is divided in two parts: upper airways, where the passage and the regulation of the airflow occur, and the lower airways, where the gas exchange occurs. The upper airways include: nasal cavities, pharynx, larynx, trachea, and bronchi.

The normal anatomy and the pathologic changes of these structures have been widely described, comparing different imaging techniques, in order to characterize the normal anatomy of these structures or the appearance of different diseases.

As reported both in human and veterinary medicine, the most effective diagnostic imaging techniques available are computed tomography (CT) and magnetic resonance imaging (MRI). These diagnostic techniques have great sensitivity in characterizing the location, extension, and relationship of the lesions with adjacent structures. This aspect is of paramount importance in planning bioptic and/or cytological sampling, and therapeutic treatments such as surgery or radiation therapy. Nevertheless, CT and MRI have a low specificity; therefore biopsy is usually required to achieve the final diagnosis.

The nasal cavities have been extensively investigated through advanced imaging techniques (CT and MRI): the normal tomographic anatomy,[1,2] and different diseases, either inflammatory/infective or neoplastic [3–7] have been characterized.

Moreover, normal anatomy and pathologic variations of different structures adjacent to the upper airway, like thyroid lobes and carotid bodies, have been studied. Secondary involvement of the pharynx, larynx, and trachea, are frequently reported due to partial occlusion or changes in their normal function.[8–16] However, to the best of authors' knowledge few information are available about the normal appearance of the pharynx [17] and imaging features of pharyngeal disease.[18–21] In veterinary literature CT and MRI are reported as a fundamental aid in the management of pharyngeal disease, particularly in conditions like oropharyngeal stick injuries, nasopharyngeal cyst or nasopharyngeal stenosis.[18–20] Instead, neoplastic diseases of the pharynx are poorly characterised.

Therefore, in this thesis we analyse the CT findings of different pharyngeal neoplasia, in order to identify features possibly differentiating tumour types. A further purpose is to characterize the regional lymphadenopathy, in order to identify features that could assess the possible nodal metastatic spread allowing an accurate staging of the patient.

1.2 GROSS ANATOMY OF THE PHARYNX

The pharynx is a unique structure because it forms the interface between the respiratory and digestive tracts.[21]

The pharynx extends approximately between a transverse plane at the level of the orbital opening, rostrally, and a transverse plane through the second cervical vertebra, caudally.[22] It may be divided into the nasal, oral and laryngeal tracts (Fig.1).

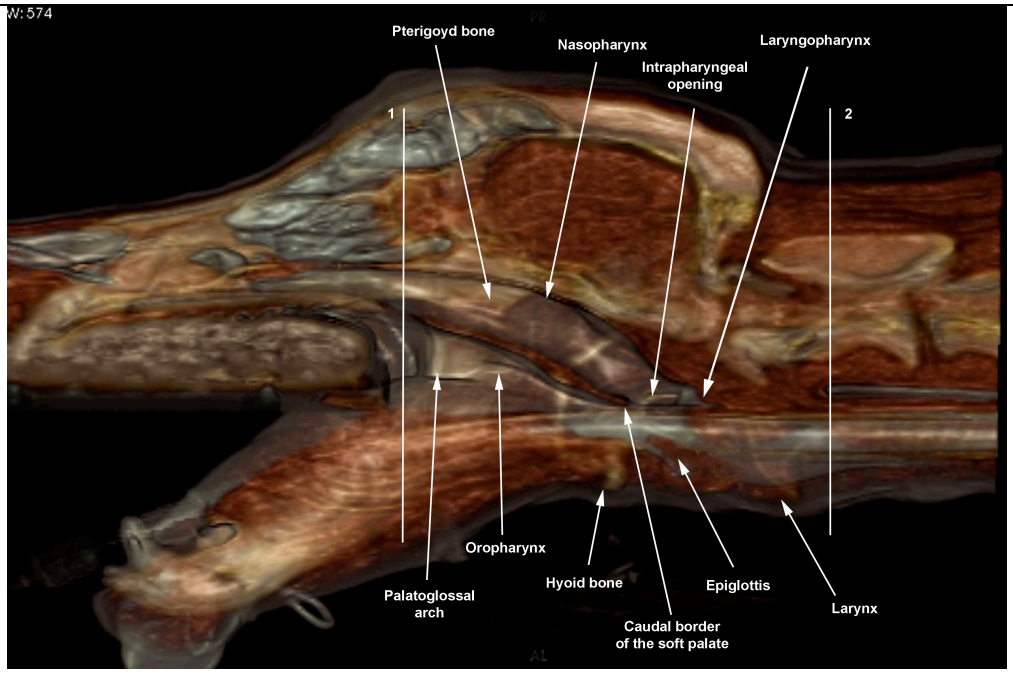

FIG. 1: 3D volume rendering, sagittal view of the head of a Dobermann dog. 1 and 2 are transverse lines passing through a plane at the level of the orbital opening and C2, respectively. These lines represent approximately the rostral and caudal limits of the pharynx.

1.2.1 Nasopharynx

The nasal pharynx extends from the choanae of the nasal cavity to the intrapharyngeal opening.[22] It is bounded ventrally by the hard and soft palate, dorsally by the vomer bone, base of the skull and muscles attached to it, and laterally by palatine bone. On each lateral wall we find the pharyngeal opening of the auditory tube, communicating with the tympanic cavity and pharyngeal and tubal tonsils, usually not grossly visible.[22] The intrapharyngeal opening is bounded by the free caudal border of the soft palate, rostrally, the palatopharyngeal arches, laterally and the laryngopharynx caudally.[22]

1.2.2 Oropharynx

The oral pharynx is located ventrally to the soft palate and dorsal to the root of the tongue, extending from the isthmus of the fauces (bounded laterally by the palatoglossal arch) to the base of the epiglottis. Just caudal to the palatoglossal arch, there is on each side the tosillar fossa, containing the palatine tonsils. The palatine tonsils have no afferent lymphatics whereas the efferent lymphatics vessels drain into the medial retropharyngeal lymph node.[22]

1.2.3 Laryngopharynx

The laryngeal part of the pharynx lies dorsal to the larynx, extending from intrapharyngeal opening, rostrally, and the esophagus caudally. The caudal limit can be identified by a transverse plane passing through the caudal border of the cricoid cartilage and the middle of the second cervical vertebra.[22] Caudo-dorsally the laryngopharynx form the piriform recess.[23] The epiglottis divides the laryngopharynx from the oropharynx.

1.3 LYMPHATIC SYSTEM

The principal lymph centres of the head are: the parotid lymph centre, the mandibular lymph centre and retropharyngeal lymph centre. Two centres in the neck drain some parts of the head also: the superficial cervical lymph centre and the deep cervical lymph centre.[24]

The **parotid lymph nodes** are located at the rostral base of the ear and drain the cutaneous area of the caudal half of the dorsum of the muzzle and the side of the cranium (the eyelids, the external ear, the temporomandibular joint and the parotid salivary gland). Furthermore they drain the temporal, masseter and zygomatic muscles; the muscles of the ear; the lacrimal apparatus; the nasal, frontal, parietal, zygomatic, and temporal bones; and the mandible. The efferent vessels of the parotid lymph nodes drain into the medial retropharyngeal lymph nodes.[24]

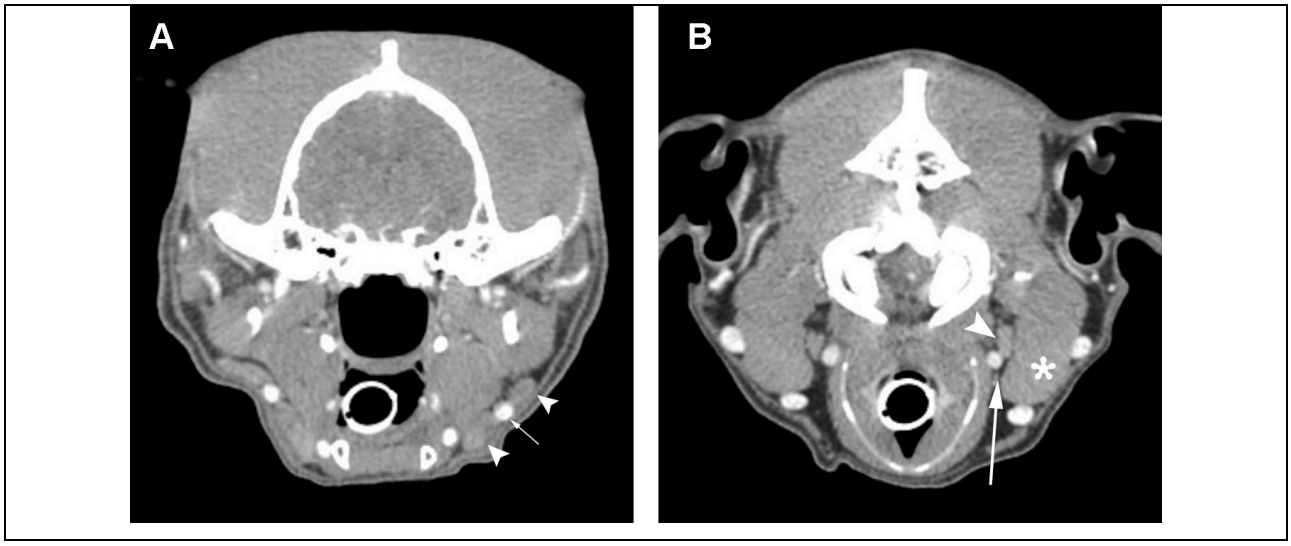

FIG. 2: A-Mandibular lymph nodes (arrow head) along the both sides of the facial vein (arrow). B- Medial retropharyngeal lymph nodes (arrow head) between common carotid artery (arrow) and mandibular salivary gland (asterisk).

The **mandibular lymph centre** include the mandibular lymph nodes (Fig. 2A) and the buccal lymph nodes, the latest could be absent. The mandibular lymph node is a group of two or three nodes located on the caudoventral aspect of the angular process of the mandible, along both sides of the facial vein[25] or linguofacial vein,[24] rostrally to the mandibular salivary gland.[26] They measure approximately 10-20 mm in length in dogs.[24] The mandibular lymph nodes receive the afferent vessels from those parts of the head not drained by parotid lymph node, but also from some overlapping areas of drainage, like eyelids, dorsum of the cranium and temporomandibular joint. A dense lymph capillary network drained the floor of the oral cavity into the mandibular lymph nodes. The efferent vessels of the mandibular lymph nodes drain primarily to the medial retropharyngeal lymph node.[24]

The **retropharyngeal lymph centre** includes a medial (Fig. 2B) and sometimes a lateral retropharyngeal lymph node. The latest is present in only the 30% of dogs.[24] The medial retropharyngeal lymph node is the largest node of the head and neck.[25] It has an elongated shape and measure approximately 5 cm length and 2 cm wide. It is located on the dorsolateral aspect of the pharynx and ventrally to the wing of the atlas, in a triangle bounded cranially by the digastric muscle, dorsally by the *longus colli* muscle and ventromedially by pharynx and larynx.[24] The *cleidocephalicus* and *sternocephalicus* muscles and the mandibular salivary gland cover the lateral aspect of the node. The common carotid artery, internal jugular vein, vagus and hypoglossal nerves course through the medial aspect of the node. All the deep structures of the head drain into the medial retropharyngeal lymph node, including oral, nasal, and pharyngeal wall, larynx and esophagus and efferent lymph vessels from parotid and mandibular lymph nodes.[24] This node receive also the primary lymph vessels directly from the palatine tonsil.[27]

The **lateral retropharyngeal lymph node** is located between the ear base and the wing of the atlas.[26] The afferent vessels come from the adjacent structures. The efferent vessels drain into the medial retropharyngeal lymph node.[24]

The pharyngeal region is drained also by the **superficial cervical lymph nodes** (Fig. 3). Two nodes

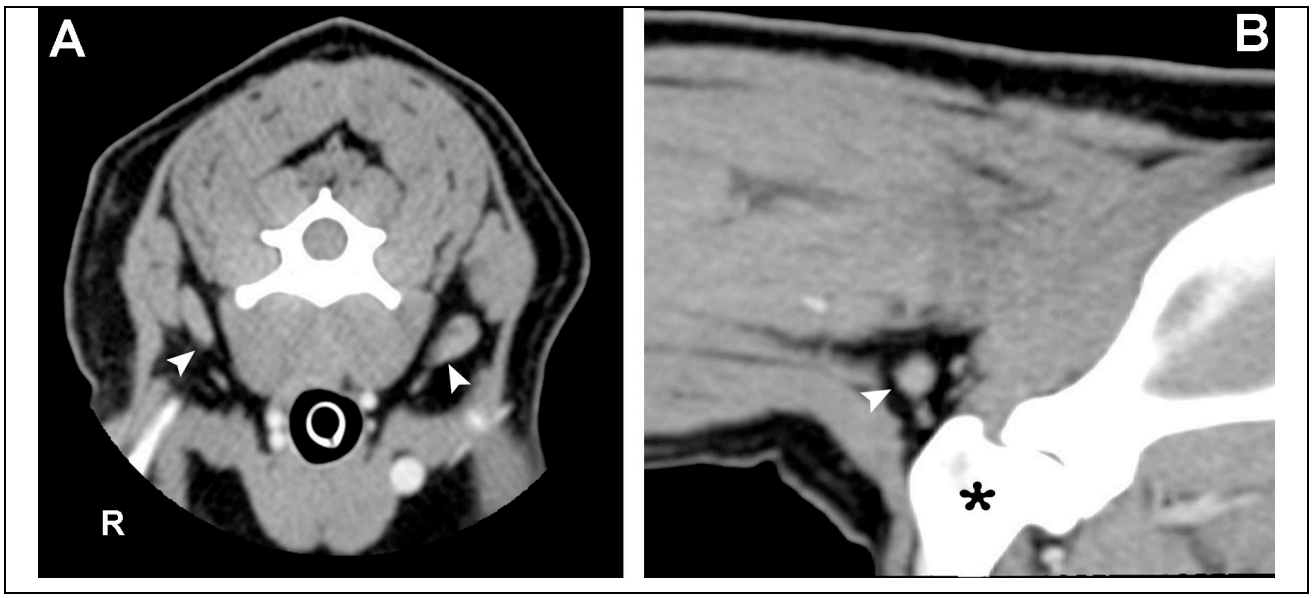

FIG 3: A- Transverse image at the level of C4, arrow heads point the superficial cervical lymph nodes. B- The lymph node is visible dorso-cranially to the great tubercle of the humerus (asterisk).

usually located cranially to the *sopraspinatus* muscle. They receive their afferent vessels from the caudal part of the head, including pharyngeal region and ear, from the lateral surface of the neck, the entire front limb, and the cranial thorax.[24] The efferent vessels go to the tracheal trunk, thoracic duct or external jugular vein.[26]

1.4 COMPUTED TOMOGRAPHIC ANATOMY

Due to the complex anatomy and the silhouetting of multiple structures of similar radiopacity, the pharynx is difficult to evaluate using radiography. To improve pharyngeal imaging evaluation, an open-mouth CT examination protocol providing better delineation of the surrounding structures has recently been proposed.[17] When the mouth is open the gas content of the lumen of the pharyngeal structures increased, particularly in nasopharynx, allowing a better visualization of the margins of the pharyngeal soft tissues. All the soft tissues of the pharynx have strong enhancement after contrast medium administration.[28]

The tonsils during the CT exam are not always clearly visible, but sometimes can be identified due to small air bubble in the tonsillar fossa. (Schwarz and Saunders, 2011) (Fig. 4).[28]

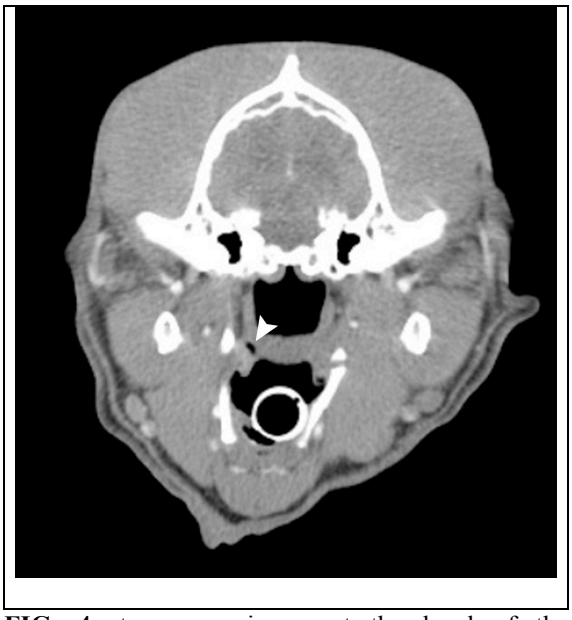

FIG. 4: transverse image at the level of the tympanic bulla. The right tonsillar fossa is highlight by the presence of a small gas bubble (arrow head) allowing to recognize the palatine tonsil.

At CT normal lymph nodes are ovoid or circular structure with homogeneous parenchyma, slightly hypoattenuating (36.6 ± 13.3 HU) compared to the muscle tissue (56.6 ± 5.8 HU). After intravenous contrast medium administration, they show homogeneous enhancement and are hyperattenuating (110.3 ± 3.3 HU) compared with muscle tissue (66 ± 4.6 HU). In some cases, an eccentric hypoattenuating area is visible, presumably the hilus.[25]

The mandibular lymph node is formed by a group of

three or four nodes, located in the transverse plane at the level of the tympanic bullae, and distributed along both side of the facial vein. The length varied from 10-25 mm.[25]

The medial retropharyngeal lymph nodes are identifiable in a triangular space bounded by the wing of the atlas dorsomedially, the mandibular gland ventrolaterally and the common carotid artery medially. The mandibular salivary gland is a consistent landmark to localize these lymph nodes. The dimension (length x height x width) is approximately 30-70 x 10 x 5-10 mm.[25]

The parotid lymph nodes is difficult to differentiate from the surrounding parotid gland and could not be identified consistently.[25]

The following figures (Fig. 5-13) illustrate the normal tomographic anatomy of the pharynx.

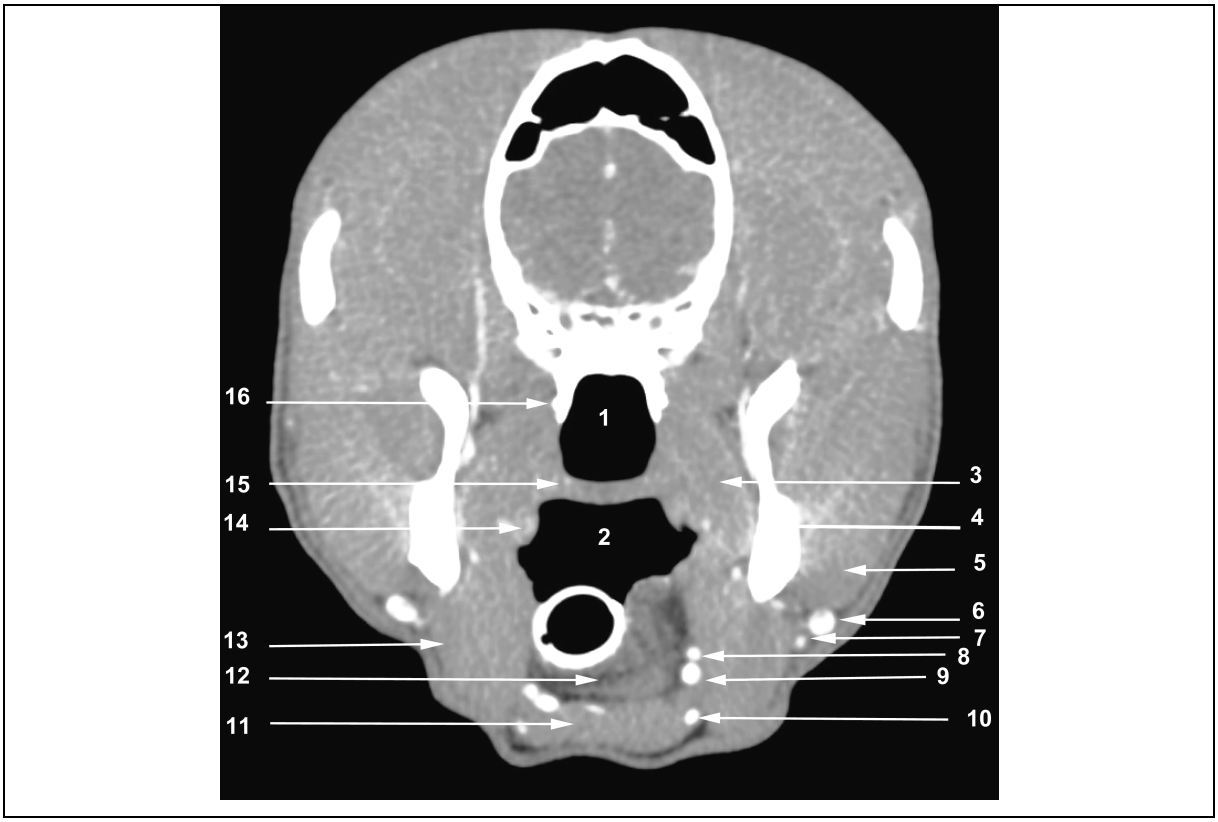

FIG. 5: 1- Nasopharynx; 2- Oropharynx; 3- Medial pterygoideus muscle; 4- Mandible; 5- Masseter muscle; 6- Facial vein ; 7- Submental vein; 8- Lingual artery; 9- Lingual vein,; 10- Sublingual vein; 11- Geniohyoideus muscle; 12- Tongue; 13- Digastric muscle;14- palatine tonsil; 15- Soft palate; 16- Pterygoid bone.

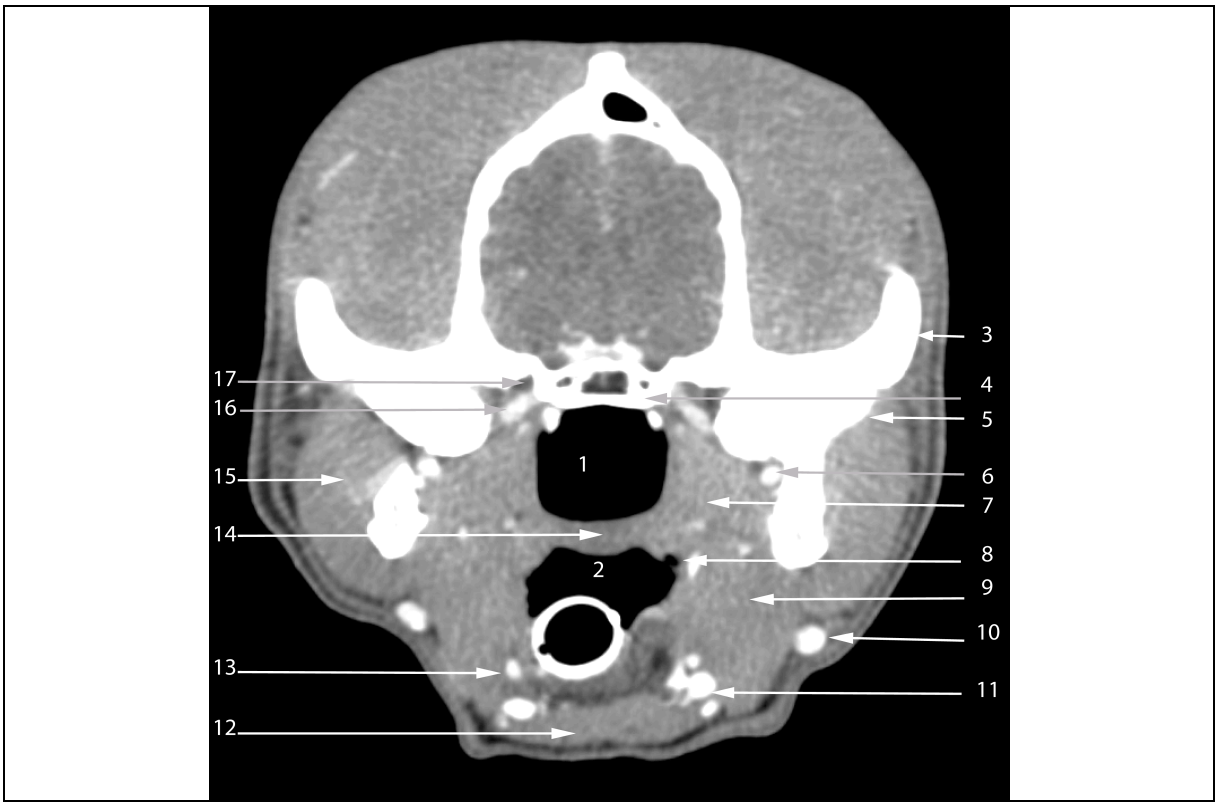

FIG. 6: 1- Nasopharynx; 2- Oropharynx; 3- Zygomatic bone; 4- Basisphenoid ; 5- Mandibular condyloid process; 6- Maxillary artery; 7- Medial pterygoideu muscle; 8- Gas bubble in the left tonsillar fossa; 9- Digastric muscle; 10- Facial vein; 11- Lingual vein; 12- Geniohyoideus muscle; 13- Lingual artery; 14- Soft palate; 15- Masseter muscle; 16- Maxillary artery; 17- Alar canal and oval foramen

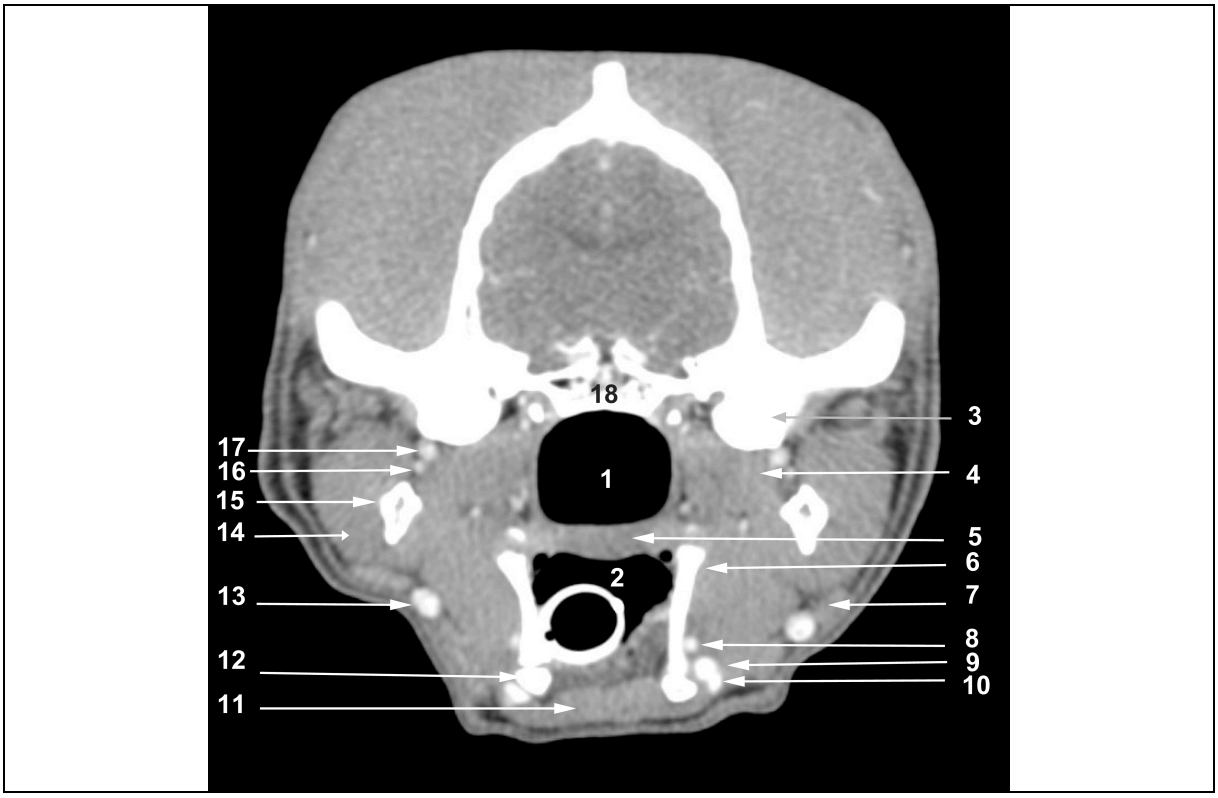

FIG. 7: 1- Nasopharynx; 2- Oropharynx; 3- Retroarticular process of the temporal bone; 4- Medial pterygoid muscle; 5- Soft palate; 6- Hyoid bone (Epihyoid); 7- Mandibular lymph nodes; 8- Lingual artery; Lingual vein; 10- Sublingual vein; 11- Geniohyoideus muscle; 12- Hyoid bone (Ceratohyoid); 13- Facial vein; 14- Masseter muscle; 15- Angular process of the mandible 16- Maxillary vein; 17- Maxillary artery; 18- Basisphenoid bone.

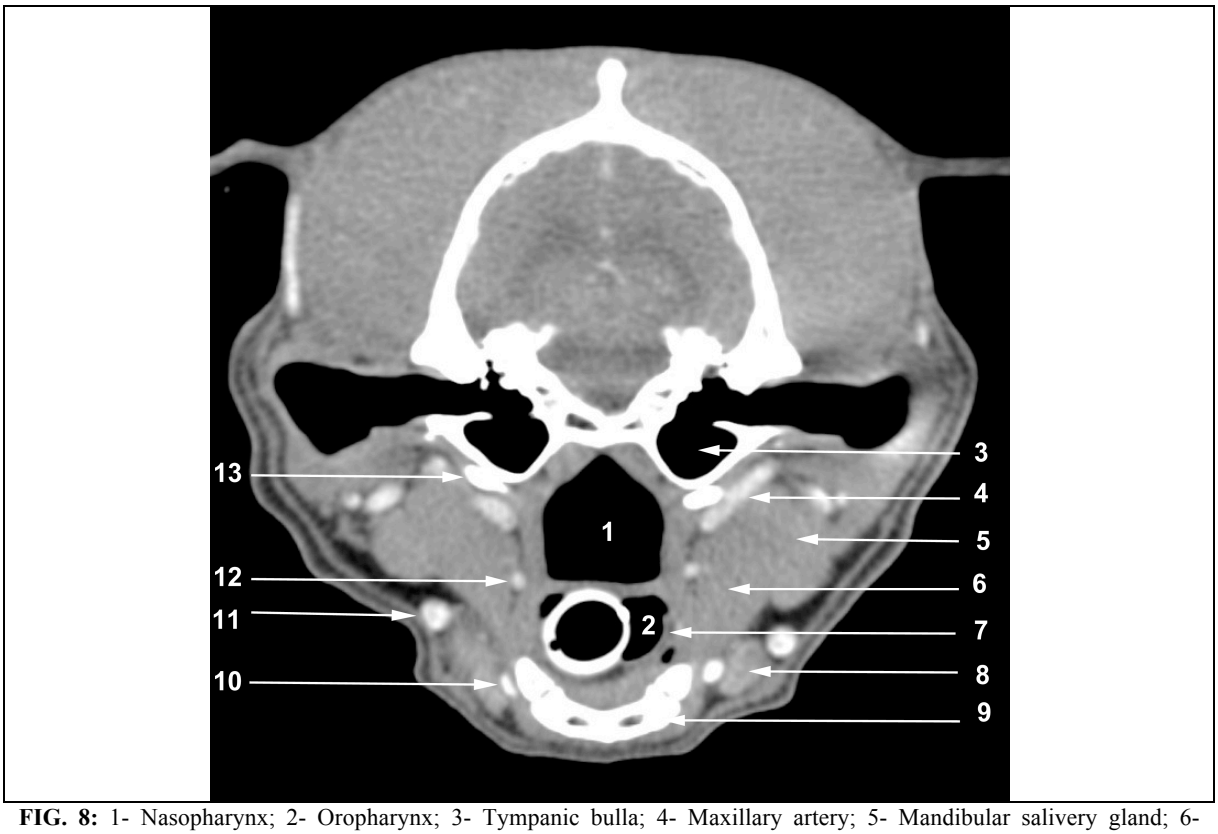

FIG. 8: 1- Nasopharynx; 2- Oropharynx; 3- Tympanic bulla; 4- Maxillary artery; 5- Mandibular salivery gland; 6- Digastric muscle; 7- Epiglottis; 8- Mandibular lymph nodes; 9- Basihyoid; 10- Lingual vein; 11- Facial vein; 12- Lingual artery; 13- Stylohyoid.

FIG. 9: 1- Oropharynx; 2- Tympanic bulla; 3- Maxillary vein; 4- Hyopharyngeus muscle; 5- Piriform recess; 6- Epiglottis; 7- Lingual vein; 8- Mandibular lymph nodes; 9- Thhyrohyoideus muscle; 10- Hyoid venous arch; 11- Epiglottic vallecula; 12- Lingual vein; 13- Facial vein, 14- Hyoid bone (Thyrohyoid); 15- Lingual artery; 16- External carotid artery; 17- Mandibular salivary gland; 18- Longus capitis muscle.

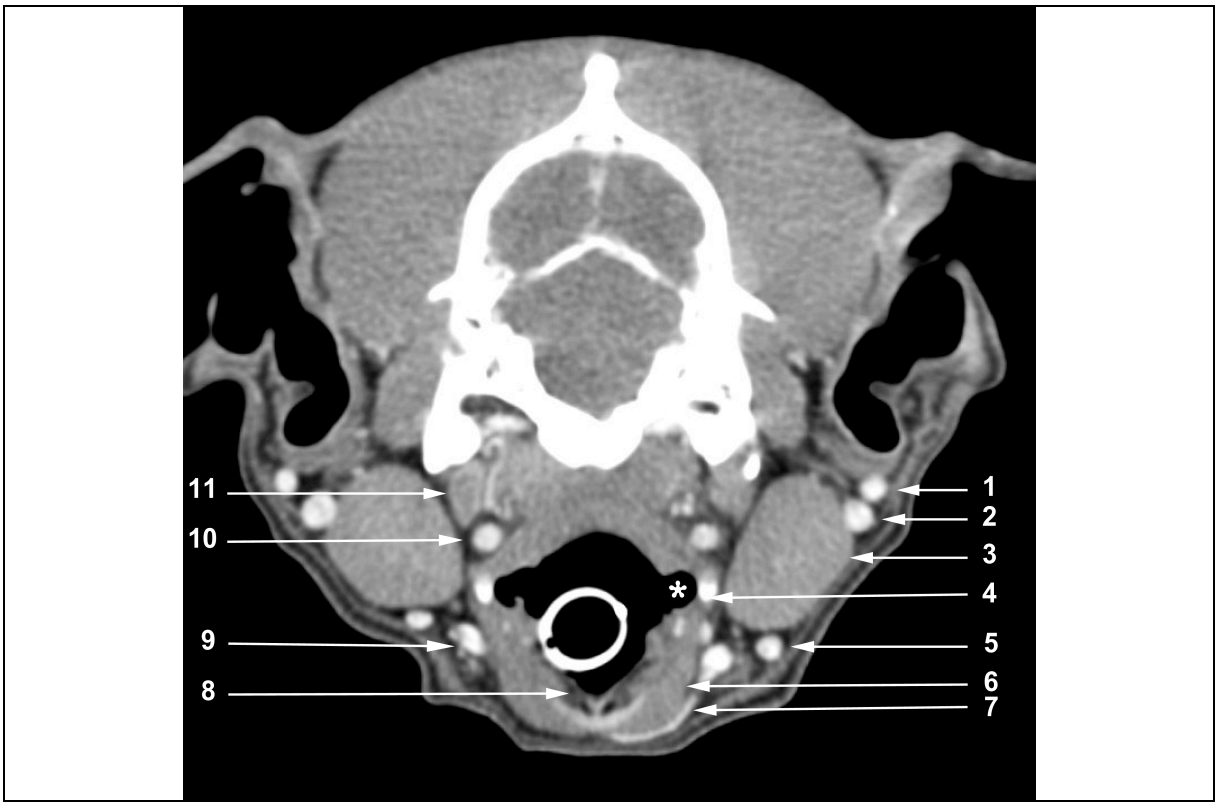

FIG. 10: *Asterisk:* Piriform recess; 1- Caudal auricolar vein; 2- Maxillary vein; 3- Mandibular salivary gland; 4- Hyoid bone (Thyrohyoid); 5- Facial vein; 6- Thyrohyoideus muscle; 7- Hyoid venous arch; 8- Epiglottis; 9- Lingual vein; 10- External carotid artery; 11- Medial retropharyngeal lymph node.

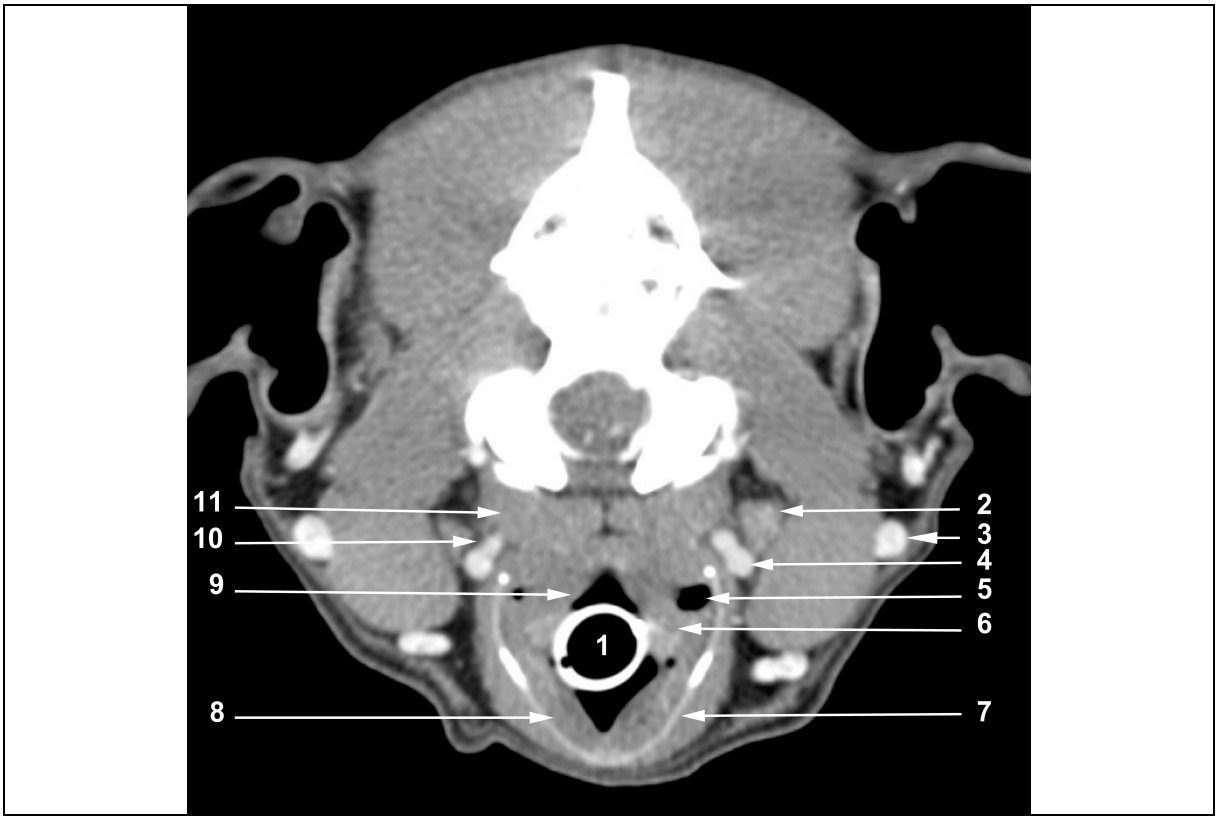

FIG. 11: 1- Laryngeal vestibule; 2- Medial retropharyngeal lymph node; 3- Maxillary vein; 4- Common carotid artery; 5- Piriform recess; 6- Aritenoid cartilage; 7- Thyroid cartilage; 8- Thyroarytenoideus muscle; 9-Ventricularis muscle; 10- Internal carotid artery; 11- Longus capitis muscle

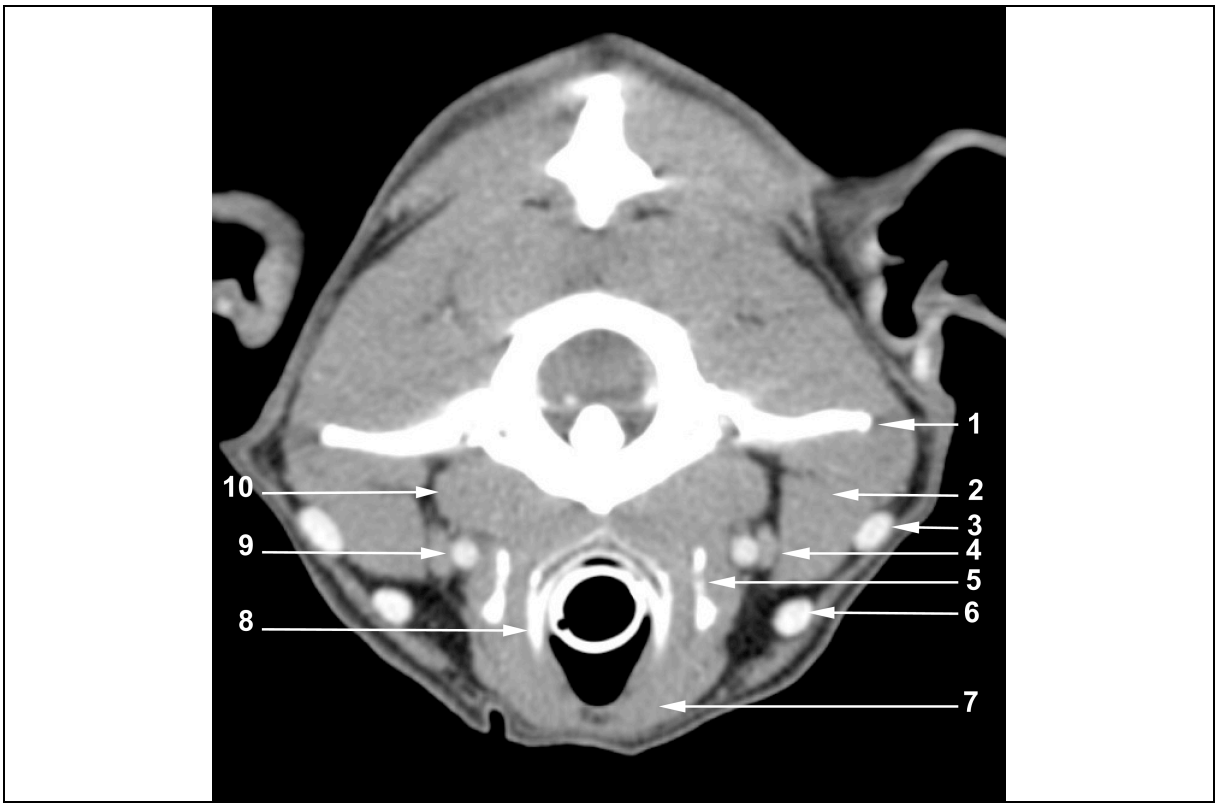

FIG. 12: 1- Atlas wing; 2- Sternomastoideus muscle; 3- Maxillary vein; 4- Medial retropharyngeal lymph node; 5- Thyroid cartilage; 6- Linguo-facial vein; 7- Sternohyoideus muscle; 8- Cricoid cartilage; 9- Common carotida artery; 10- Longus capitis muscle

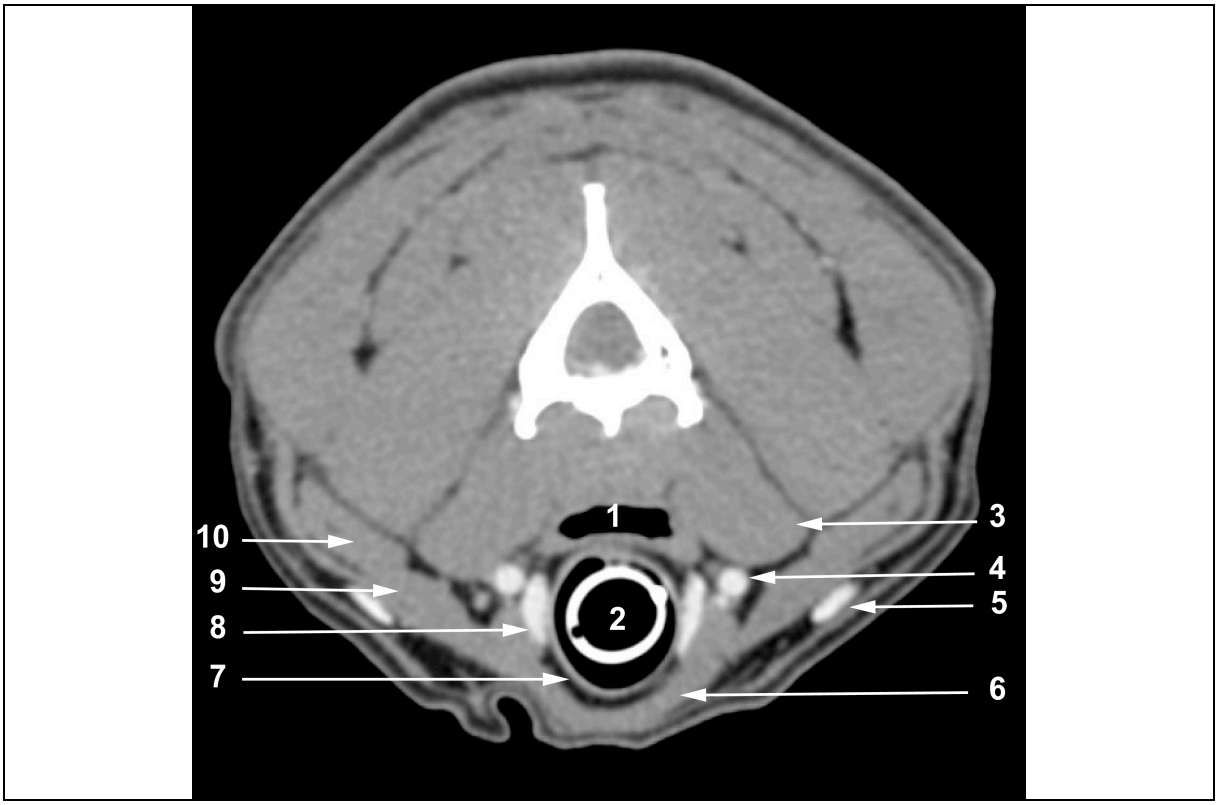

FIG 13: 1- Esophagus; 2- Trachea; 3- Longus capitis muscle; 4- Common carotid artery; 5- Jugular vein; 6- Sternohyoideus muscle; 7- Tracheal ring; 8- Right thyroid lobe; 9- Sternomastoideus muscle; 10- Brachiocephalicus muscle.

CHAPTER 2

PHARYNGEAL DISEASES

This chapter was adapted from: Carozzi F, Zotti A, Alberti M, Rossi F. Computed tomographic features of pahreyngeal neoplasia in 25 dogs. *Veterinary Radiology and Ultrasound 2015; 56 (6); 628-637.*

2.1 INTRODUCTION

The pharynx is the common interface between digestive and respiratory tracts. Due to its anatomical location, pharyngeal disease may present clinical signs referable to upper respiratory tract (stertor, open mouth breathing, snoring, sneezing, cough, nasal discharge) or digestive tracts (gagging, dysphagia, retching, ptyalism, regurgitation, and vomiting).[21]

The oral and oropharyngeal cavity of the dog are very common sites of various canine malignant and benign neoplasia,[29] representing the fourth most common location of malignant neoplasia in the dog.[30–32] The biologic and epidemiologic behaviour of these tumours in the dog have features overlapping with the human cancer. In humans head and neck cancers account for 3% to 4% of malignant neoplasia.[33] The male to female ratio, for head and neck cancers, is 2:1 and the squamous cell carcinoma (SCC) represents the 90% of cancers of head and neck.[33] Similar data are reported in veterinary medicine, where male dogs have a 2.4 times greater risk of developing pharyngeal malignancy compared to female dogs[30,31,34,35] except in malignant melanoma, where a gender predisposition has been inconsistently reported.[30,34,36]

Dogs develop spontaneous tumours twice as frequently as humans, with histopathologic and biologic behaviour similar to tumours occurring in human. The biologic and epidemiologic behaviour of different tumours are influenced by a number of variables, like age, breed, sex, and also the geographic location.[29] It has been theorized that dogs living in metropolitan area are exposed to numerous environmental carcinogens (like air pollutants) that could significantly influence the occurrence of certain type of neoplasia like tonsillar carcinoma, melanoma or nasal tumour. These factors along with the relative shortness of the life span of the dog, and the intimacy with which this species shares the man's environment makes the dog an excellent animal model for comparative epidemiologic studies.[30,35,37]

The incidence rate of canine primary pharyngeal tumours varies in relation to the affected area. In the dog, the most common tumours of the oropharyngeal tract are, in descending order, malignant melanoma, SCC, and fibrosarcoma,[30–32,34,38] although SCC is more common than malignant

melanoma in other studies.[30,34] The palatine tonsil is the most common site for SCC.[31,32,37] Primary nasopharyngeal and laryngopharyngeal tumours are instead rare in dogs.[39–41] Nasopharyngeal masses are often nasal adenocarcinoma with secondary nasopharyngeal involvement.[29,41] The most common laryngopharyngeal tumour is SCC.[39,40] Distinction between nasopharyngeal, oropharyngeal and laryngopharyngeal disorders based on CT imaging techniques is challenging because any lesion may overlap adjacent areas.

In humans use of cross sectional imaging such as CT and magnetic resonance imaging, plays the role of identifying the likely origin, extent of lesions and to assess the no palpable lymph nodes,[33,42] but the imaging findings have little specificity.[43] However, computed tomographic imaging is a fundamental part of the diagnostic work-up in neoplastic diseases, not only for the diagnosis, but also for staging and planning therapy. Some pharyngeal tumours, such as malignant melanoma and tonsillar squamous cell carcinoma (TSCC), can have a particularly aggressive biological behaviour,[30] influencing prognosis and treatment planning.

2.2 MALIGNANT MELANOMA

Melanoma is the most common oral malignant neoplasia in the dog.[36] It arises from melanocytes, which are cells that generate pigment through the melanosome. Malignant melanoma tends to occur in smaller dogs, and is most commonly diagnosed in breeds like Scottish terrier, golden retrievers, poodles, and dachshund.[30] It does not show a gender predilection and is primarily a disease of the older dogs.[36] The localizations of oral melanoma are, in order of decreasing frequency: gingiva, lips, tongue, and hard palate.[30]

Many factors determine the biological behaviour of this tumour, the primary are anatomic site, size, stage and histologic parameters. The anatomic site is highly predictive of local invasiveness and metastatic propensity, but location alone cannot be used to predict prognosis. Melanoma involving the haired skin, often has a benign behaviour.[30] Oral and/or mucosal melanoma are considered extremely malignant tumour. Differential neoplastic diagnosis includes squamous cell carcinoma,

fibrosarcoma, epulides and odontogenic tumours and others. The size of lesions at the moment of diagnosis is extremely prognostic, and the World Health Organization staging scheme is based on size, with Stage I= < 2 cm diameter-tumour, Stage II= 2 cm to <4 cm diameter-tumour, Stage III= 4 cm o grater tumour with or without nodal metastasis, and Stage IV= distant metastasis. However this staging scheme is not standardized to the size of patient. Thus other prognostic factors have been proposed as alternative staging system by other studies. Size is always considered extremely prognostic, other factors are: lesser degree of extirpation and incomplete surgical margins; location (caudal mandibular and rostral maxillary regions have poor prognosis); tumour mitotic index > 3; and bone invasion/lysis.[36] Staging, include complete blood count, platelet count, biochemical profile, urinalysis, three-projection chest radiography, abdominal ultrasound and local, bilateral, lymph node aspiration, also if lymphadenomegaly is not present. This is important because as reported by Williams and Packer in 2003, about 70% of dogs with oral melanoma have metastasis in enlarged lymph node, but about 40% of dogs had metastasis when no lymphadenomegaly was present.[44]

2.3 SQUAMOUS CELL CARCINOMA

Squamous cell carcinoma (SCC) is the second most common oral tumour in the dog and the most prevalent oral malignancy in humans.[38] Tonsillar SCC tends to occur in small breed dogs, whereas non-tonsillar SCC tends to occur in large breed dogs.[31].

The oral SCC can be divided into three groups according to location and biological behaviour: tonsillar; non-tonsillar or gingival; and SCC of the tongue, palate and pharynx.[37] The rostral cavity SCC has a low metastatic rate, reported in up to 5%-10 % to the regional lymph nodes and 3% to 36% for distant metastasis.[31] The caudal tongue and tonsil have a higher metastatic potential,[30] particularly tonsillar SCC has been reported to metastasise to the regional lymph nodes in 77% of cases, and in 42% to 63% in distant sites.[30] Tonsillar SCC is 10 times more common in animal living in urban rural areas. Differential neoplastic diagnosis for tonsillar lesion could be: lymphoma,

usually bilateral and accompanied by multicentric lymphadenopathy; malignant melanoma, often metastasise to the tonsils. Cervical lymphadenopathy is common. Even if disease appear to be confined to the tonsil, this disease is considered systemic at diagnosis in over 90% of dogs and is often bilateral, so tonsillectomy should be done bilaterally.[30] The prognosis for tongue tumours depends on the site, type, and grade of cancer. Tongue SCC grading base on histologic features such as differentiation, keratinization, mitotic rate, tissue and vascular invasion, nuclear pleomorphism, and scirrhous reaction.[30] Cancer of the rostral tongue has better prognosis, because are detected in earlier stage and are easier to resect with wide margins, whereas cancer of the caudal tongue are more difficult to visualize, to achieve aggressive resection and further this part of the tongue is rich in lymphatic and vascular vessels allowing metastatic spread.

Few reports on computed tomographic (CT) findings of oral SCC have been published in dogs and cats.[45,46]

2.4 FIBROSARCOMA

Oral fibrosarcoma is the third most common oral tumour in dogs. Young large breed dogs are the most represented, particularly golden and Labrador retrievers, with a median of 7.3 to 8.6 years; with a possible male predisposition. Fibrosarcoma is locally aggressive but has low metastatic risk to lungs or regional lymph nodes, with metastases reported, respectively, in 27% and in 19% to 22% of dogs.[30] The local infiltration is more problematic than metastases because it renders most of these lesions inoperable,[37] making the radiation therapy and/or chemotherapy the most useful tools. The prognosis for canine soft tissue sarcoma depends on histologic type, degree of cellular differentiation, number of mitotic figures, location, and success of complete surgical excision.[29] Sarcomas in the dog and cat are good models to study the therapeutic approaches for humans soft tissue sarcomas.[29]

CHAPTER 3

STAGING

3.1 TNM SYSTEM

The term *staging* refers to the evaluation and categorization of the oncologic patients into groups accordingly to the clinical extent of their malignancy, after the systematic assessment of the prognostically-significant features of the primary tumour (T), the regional lymph nodes (N), and presence of distant metastases (M),[47] the so-called tumour-node-metastasis (TNM) system. This system provides an objective description of the clinical extent of the neoplastic disease, helping to determine the prognosis and treatment plan.[47] This system was first reported by Pierre Denoix in the 1940s, then adapted in 1968 by the International Union Against Cancer (UICC) which compiled the first edition of the TNM staging for 23 body sites.[48] Over the years, TNM system has been reviewed and improved aided by advances in medical technology that allowed a better assessment of the extent of tumours. The first edition of TNM classification of tumours of domestic animals is dated 1980.[49] In the following Tables 1 and 2 the TNM classification about canine oropharyngeal tumours and nasal chambers, including nasopharynx, is reported.

Table 1: WHO Clinical stage (TNM) of Canine tumours of the Oropharynx[49] (Owen et al 1980)

T:	**Primary tumour**	
Tis	Carcinoma in situ	
T0	No evidence of primary tumour	
T1	Tumour superficial or exophytic; maximum diameter < 2cm	
	T1a without systemic signs	**T1b** with systemic signs
T2	Tumour with invasion of tonsil only; maximum diameter 2 to 4 cm	**T2b** with systemic signs
	T2a without systemic signs	
T3	Tumour with invasion of surrounding tissue; maximum diameter > 4cm	**T3b** without systemic signs
	T3a without systemic signs	
	Ta without evidence of bone invasion	
	Tb with evidence of bone invasion	
N:	**Regional Lymph Nodes (RLN)**	
N0	No evidence of RLN involvement	
N1	Movable ipsilateral nodes	
	N1a absence of metastases*	**N1b** presence of metastases*
N2	Movable counterlateral or bilateral nodes	
	N2a absence metastases*	**N2b** presence metastases*
N3	Fixed nodes	
M:	**Distant metastasis**	
M0	No evidence of distant metastasis	
M1	Evidence of distant metastasis	

* presence or absence of metastases is histologically confirmed

Table 2: WHO Clinical stage (TNM) of Canine tumours of the Nasal Chambers and Sinuses[49] (Owen et al 1980)		
T:	**Primary tumour**	
T0	No evidence of primary tumour	
T1	Tumour ipsilateral with minimal or bone lysis	
T2	Tumour bilateral and/or moderate bone lysis	
T3	Tumour with invasion of surrounding tissue	
N:	**Regional Lymph Nodes (RLN)**	
N0	No evidence of RLN involvement	
N1	Movable ipsilateral nodes	
	N1a absence of metastases*	**N1b** presence of metastases*
N2	Movable counterlateral or bilateral nodes	
	N2a absence metastases*	**N2b** presence metastases*
N3	Fixed nodes	
M:	**Distant metastasis**	
M0	No evidence of distant metastasis	
M1	Evidence of distant metastasis	
* presence or absence of metastases is histologically confirmed		

The evaluation of the primary tumour (T) is based on assessment of the extent of the tumour, considering size criteria and degree of local infiltration of soft or bony tissues. Assessment of the local and regional lymph nodes (N) focuses on the presence of metastasis in the ipsilateral and/or counterlaterals lymph nodes. Distant metastasis status (M) indicates the absence or presence of distant metastases. Within each category a progressive number is assigned based on clinical, different diagnostic imaging techniques (radiography, ultrasound, CT or MRI), and histopathologic evaluation.[50] Increasing number indicate increasing extension of tumour, and progressive nodal or systemic involvement.

The potential combination of T, N, and M are multiple, but for practical purposes the various combination have been grouped in four major staging groups (Stages I-IV), from the least to most advanced tumour (Table 3).[47] The advantage of the staging is determine the therapeutic workup and the prognosis on the basis of the extent of the malignancy.

Computed tomography is a valuable tool in the evaluation of head and neck tumour in human. Its high sensitivity may change dramatically the tumour stage, with both tumour and nodal staging affected.[51] The presence of ipsilateral or bilateral metastatic lymphadenopathy is an important

prognostic factor in patients with squamous cell carcinoma, reducing dramatically the projected survival time.[52]

Table 3: Stage Grouping for the pharynx neoplasia[49] (Owen et al 1980)			
Stage	**T**	**N**	**M**
I	T1	N0, N1a or N2b	M0
II	T2		M0
III	T3	N0, N1a or N2a	M0
	Any T	N1b	
IV	Any T	Any N2b or N3	M0
	Any T	Any N	M1

3.2 LYMPH NODES ASSESSMENT

In human medicine the critical information to the treatment and prognostic assessment in patients affected by head and neck cancer is the evaluation of cervical nodal metastatic disease. Sole palpation of lymph nodes is not highly reliable, being limited to superficial lymph nodes. Also in veterinary medicine the clinical evaluation of lymph nodes in case of head and neck cancer is limited to superficial lymph nodes like mandibular lymph nodes or superficial cervical lymph nodes, whereas other important lymph centres, like medial retropharyngeal lymph nodes are not evaluable. Thus the evaluation of these lymph nodes by cross sectional imaging technique (CT or MRI) is essential for the complete staging of the oncologic patient. The principals imaging criteria for the evaluation of the lymphadenopathy on CT are considered: the size, the shape, presence of central necrosis, extracapsular spread, and carotid artery and/or skull base invasion.[33,53–56]

In human medicine, *size* criterion consider a greater longitudinal diameter of 1.5 cm for the jugulodigastric and submandibular nodes and 1 cm for all other cervical nodes indicative for presence of metastasis. If the minimal axial parameter is considered, a diameter of 1.1 cm for jugulodigastric lymph nodes and 1 cm for all other cervical nodes is considered indicative of abnormality.[53] In veterinary medicine the range of nodal dimensions is wider due to extreme variation in size and shape of canine head.[25] So an absolute size cut off may be an inaccurate criterion for evaluation of nodal metastasis[57] and should be regarded cautiously. In a recent study

were compared the MRI features occur more likely in inflammatory adenopathy and neoplastic adenopathy. Lymphadenitis has moderate to marked perinodal contrast enhancement, and muscle contrast enhancement, whereas larger, nonpainful mass lesion is indicative of neoplastic lesion.[58]

Nodal *shape* is not specific but benign nodes tend to have kidney bean or flat shape, whereas malignant nodes tend to be rounded.

The most accurate CT criterion is *central necrosis.*[54] A benign node usually present fat at the level of the hilus, which may be distinguished from necrosis by its location at the periphery of the node, whereas necrosis occurs centrally, with density similar to the surrounding fat tissue of the neck.[33] Actually, initially tumour cells replace the medulla of the node, and after this necrosis of medulla occur. Thus, hypoattenuating medullary area of the node contains both tumour cells and necrosis,[54,56] and it is surrounded by a thick rim of residual enhancing lymphatic tissue.[33] The incidence of central necrosis is reported to be directly proportional to the size of the nodes.[56] If the internal attenuation area has the density resembling the density of water on CT the term *cystic adenopathy* may be apllied.[53]

In CT the *extracapsular spread* is the extension of metastatic tumour beyond the lymph node capsule and may be suspected when there are poorly defined margins or there is soft tissue infiltration or stranding of muscle or fat of the neck.[33] These criteria are accurate if there has been no recent infection, radiation therapy, or surgical intervention in the same area. The incidence of extracapsular spread increases as lymph node size increases.[56] In human medicine the presence of extracapsular spread portends for a poor prognosis.[59]

Grouping is the presence of a group of contiguous and confluent lymph nodes in the draining chain of a tumour, which has a maximal diameter of 8-15 mm, and is highly indicative of metastatic disease.[54]

Once the presence of nodal metastases has been established, other important features impact on the prognosis and management of the patient. Specifically the carotid artery encasement and eventual extension or fixation to the skull base, influence the operability of the patient and the prognosis.

The carotid encasement is assessed by evaluating the fatty interface between the tumour and the vessel wall, and how many of the circumference of the vessel is surrounded by tumour (<180 degree usually indicates absence of invasion; involvement of 270 degrees or more is predicted of wall invasion).[33] Identification of tumour extension to the skull base, laryngeal cartilage erosion or invasion of vertebral compartment, has the worst prognosis (Fig. 14).[33]

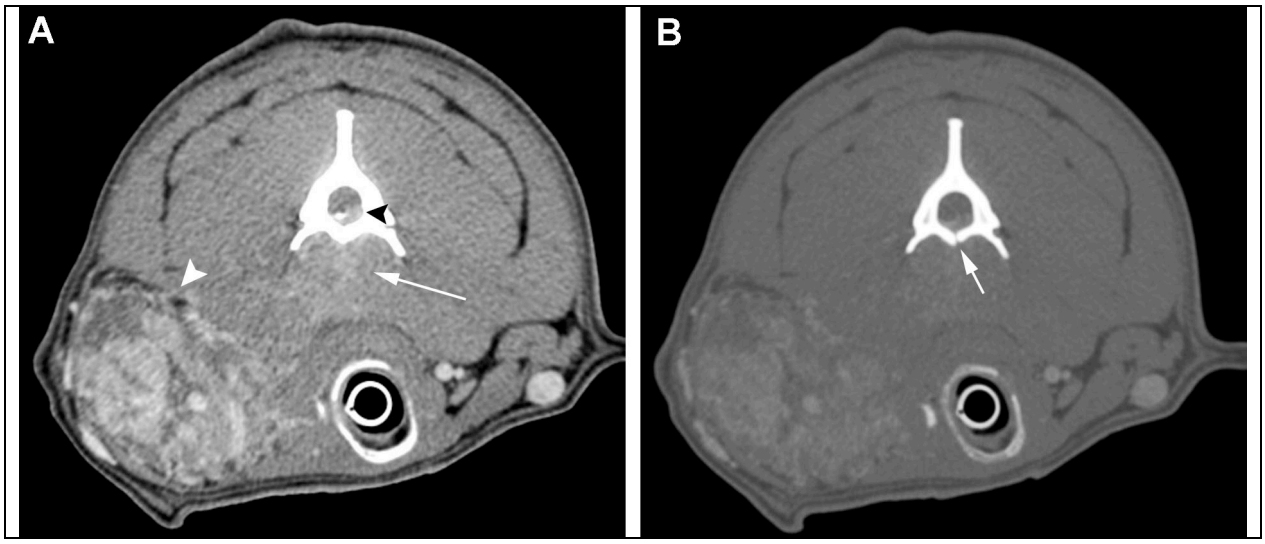

FIG. 14: Transverse soft tissue window (A) and bone window (B), post-contrast CT images. Dogue de Bordeaux, male, 8 years old, diagnosed with a malignant epithelial neoplasia. A soft-tissue window: heterogeneous, ill-defined space occupying lesion (arrow head) on the right of the larynx. The enhancement extends dorsomedially reaching the ventral margin of C2 (arrow). In this section is visible a soft tissue enhancement in ventral portion of the vertebral canal compatible with neoplastic invasion. B: the arrow shows a small lytic lesion in the body of the axis, a possible route of invasion of the vertebral canal.

CHAPTER 4

MATERIALS AND METHODS

This chapter was adapted from: Carozzi F, Zotti A, Alberti M, Rossi F. Computed tomographic features of pahreyngeal neoplasia in 25 dogs. *Veterinary Radiology and Ultrasound 2015; 56 (6); 628-637.*

4.1 STUDY POPULATION

Medical records and CT studies of dogs presented with primary neoplasia of the nasopharyngeal, oropharyngeal and laryngopharyngeal tracts were collected from the databases of three reference centre for diagnostic imaging: Clinica Veterinaria dell'Orologio (Sasso Marconi, Bologna, Italy, n=15), Veterinary Hospital "I Portoni Rossi" (Zola Predosa, Bologna, Italy, n=9) and Clinica Veterinaria Pedrani (Zugliano, Vicenza, Italy, n=1).

The inclusion criteria were the presence of either histological or cytological diagnosis of the lesions and the availability of a pre- and post-contrast CT images of the head. The absence of a pathology report indicating the definitive neoplastic origin and type of neoplasia, leads to exclusion of the case from the study. Diagnosis confirmation was achieved histologically by excisional biopsy, or by *in vivo* core needle biopsy, and cytologically by the fine needle aspiration (FNA) technique. Presence of nodal metastasis was verified by FNA or core needle biopsy. The acquisition method for core needle biopsy or FNA was: by palpation if lymph nodes were markedly enlarged, ultrasound-guided if they were slightly enlarged.

4.2 COMPUTED TOMOGRAPHIC IMAGING

The CT images were acquired using either a multidetector CT (n=16) or a single-slice helical-CT [SSCT] (n=9). All dogs underwent general anaesthesia and were positioned in sternal recumbency. Since this was a retrospective multi-institutional study, the acquisition protocols were not standardised: they included pre- and post-contrast series, slice thickness ranging between 1.25 and 5 mm, and a matrix size of 512x512. FOV ranged between 200 and 250 mm, kVp varied from 100 to 140 and mAs from 80 to 230, while pitch ranged between 0.562 and 1.75. Post-contrast series were obtained after injection of a bolus of intravenous water-soluble iodinated contrast medium (Optiray 300 mg/ml, COVIDIEN, Segrate, MI, Italy) at a dose of 600 mg/kg. Image analysis was performed on soft tissue and bone reconstruction algorithms.

4.3 IMAGE ANALYSIS

All CT images were analysed by three investigators, one of whom is a board-certified radiologist, and the CT features were recorded by consensus. Observers were aware of the final diagnoses at the time of CT images revision.

All computed tomographic images included in this study were reviewed, analysed and measurements were taken using an open-source dedicated DICOM viewer software (OsiriX 4.1.2, 32 bit, Pixmeo, Switzerland). Window settings were adjusted as needed. A multi-planar reconstruction (MPR) software tool was used to characterize the lesions. One reader performed all measurements three times for each case, and then the mean values were averaged within each group. Imaging characteristics recorded were divided in two groups: qualitative and quantitative criteria. **Qualitative CT image criteria** included: presence and location of mass/nodular lesions or tissues thickening in the nasopharyngeal, oropharyngeal and laryngopharyngeal tracts. Lesion shape was subjectively defined as round, oval or irregular; whereas lesion margins were classified as well-defined, if a distinct border to the surrounding tissues could be detected after contrast administration, or ill-defined. There was also assessment of the relationship with adjacent tissues/structures, including presence of mass effect (displacement of surrounding tissues/structures) and/or infiltrative growth. The pre-contrast appearance of the lesion was subjectively defined as homogenous or heterogeneous, and contrast enhancement, was defined as homogenous, heterogeneous or peripheral (rim enhancement). Furthermore, the grade of contrast enhancement was subjectively evaluated as mild, moderate or marked. The presence of hypoattenuating non-enhancing areas as well as areas of calcification was recorded. Lymphadenopathy was documented when the medial retropharyngeal and mandibular lymph nodes had bilateral or monolateral enlargement and it was subjectively evaluated as mild, moderate, or marked. Regional lymph nodes shape were recorded and classified as round or elongated and contrast enhancement of the regional lymph nodes was recorded as homogeneous or heterogeneous. The relationship with surrounding vessels (common and external carotid arteries, jugular veins, lingual and facial arteries and veins) was evaluated on the basis of

displacement of vessels by the mass, vessel inclusion within the mass or evidence of an intraluminal defect in a post-contrast series.

The presence of potential distant metastases was recorded by total body CT, head and thorax CT or by radiographs of the thorax in one case, when pulmonary nodules, or nodular lesions in other organs were observed. Equivocal findings were discussed in collegial session and final decision was reached by consensus.

Quantitative CT image criteria included: volume of the mass was measured with the rotational ellipse method (max. height x max. width x max. length x $\pi/6$). Pre- and post-contrast attenuation values expressed as Hounsfield Units (HU) were measured. Overall lesion attenuation was calculated by selecting three different ROI, as large as possible, in three different parts of the lesion, with one each at the cranial, middle and caudal aspects of the mass, on the pre- and post-contrast series. The mean HU and standard deviation (SD) values in the pre- and post-contrast series in the three areas were calculated.

4.4 STATISTICAL PROCEDURES

Statistical analysis was performed by a statistical consultant (Barbara Contiero, University of Padova). To test the effect of final diagnosis (carcinoma vs. sarcoma vs. melanoma), data were compiled in an Excel spreadsheet (Microsoft Corporation, 2007, USA) and analysed by a commercial statistical software (SAS 9.3, SAS Inc., Cary, NC). Shape, margins and enhancement grade of lesions as well as enlargement, shape and enhancement of lymph nodes were assessed using a one-way non-parametric ANOVA statistical model (Kruskal-Wallis' Test). The continuous variables, such as volume and pre- and post-contrast lesion attenuation, were assessed by means of a one-way ANOVA statistical model. Incidence of pharyngeal malignancy in relation to gender and the relationship with adjacent tissues was assessed by *z* test, whereas the pre-contrast aspect and distribution pattern of contrast medium were assessed by means of the Chi-squared test. Furthermore, the association between subjective evaluation of those lymph nodes presenting a

markedly enlarged, rounded shape and with heterogeneous enhancement, and the actual presence of nodal metastasis, assessed by cytology or histology, was analysed using Fisher's Exact Test.

A P-value of less than 0.05 was deemed to be statistically significant.

The single case of pharyngeal lymphoma was excluded from the statistical analysis.

CHAPTER 5

RESULTS

This chapter was adapted from: Carozzi F, Zotti A, Alberti M, Rossi F. Computed tomographic features of pahreyngeal neoplasia in 25 dogs. *Veterinary Radiology and Ultrasound 2015; 56 (6); 628-637.*

5.1 PATIENT POPULATION

The study population mean age (±SD) was 9.56 ±3.16 years (+3-14 years). Breed, age and gender distribution are summarised in Table 4.

Table 4: Signalment of 25 Dogs with Pharyngeal Tumours.

	Breed	Age (years)	Sex
CARCINOMA			
- **TSCC * (7)**	Mongrel (4)	10; 8; 6; 6	Male (5)
	Border Collie (2)	10; 14	Female (2)
	Labrador Retriever	12	
- **Non-TSCC† (2)**	French Bulldog	11	Male
	Maltese	12	Female
- **Tonsillar carcinoma (3)**	Springer Spaniel	7	Male (3)
	Labrador Retriever	7	
	West Highland White Terrier	12	
- **Adenocarcinoma (3)**	French Bulldog	10	Male (2)
	Beagle	10	Female
	Boxer	8	
SARCOMA			
- **Histiocytic Sarcoma (2)**	Jack Russell (2)	3; 3	Male (2)
- **Fibrosarcoma**	Beagle	7	Male
- **Undifferentiated Sarcoma**	Mongrel	13	Female
- **Extraskeletal Osteosarcoma**	Border Collie	8	Female
MELANOMA	Mongrel	14	Male
	Cocker Spaniel	12	Female (3)
	Golden Retriever	14	
	Rottweiler	11	
LYMPHOMA	Bull Terrier	11	Female

*TSCC= Tonsillar Squamous Cell Carcinoma
†Non-TSCC= Non-Tonsillar Squamous Cell Caricnoma

Tumour types included in this study were: 15 carcinoma (TSCC [n=7, two of these cases were in the same dog, one was the first presentation and the other was a recurrence after surgical debulking] (Fig. 15A-C), non-tonsillar SCC (non-TSCC) [n=2], tonsillar carcinoma [n=3] (not further classified), adenocarcinoma [n=3]); 5 sarcomas (histiocytic sarcoma [n=2], fibrosarcoma [n=1], undifferentiated sarcoma [n=1], extraskeletal osteosarcoma [n=1]); 4 malignant melanomas; and 1 lymphoma. Histologic diagnosis was obtained in 16 dogs (13 core needle biopsies and 3 excisional biopsies), and cytologic diagnosis in 9 dogs.

Eighteen dogs had total body CT, 6 dogs had head and thorax CT, whereas 1 dog had CT of the head and ventro-dorsal and two lateral radiographs of the thorax.

The CT findings are summarised in Table 5.

Table 5: CT Features of the Carcinomas, Sarcomas, Melanomas and Lymphoma				
	Carcinoma n=15	**Sarcoma n= 5**	**Melanoma n=4**	**Lymphoma n=1**
LOCATION				
- Oropharynx	13/15 (87%)	4/5 (80%)	4/4 (100%)	1/1 (100%)
- Laryngopharynx	4/15 (27%)	2/5 (40%)	1/4 (25%)	1/1 (100%)
- Nasopharynx	2/15 (13%)	-	-	-
SHAPE				
- Round	0/15 (0%)	-	-	-
- Oval	6/15 (40%)	-	-	-
- Irregular	9/15 (60%)	5/5 (100%)	4/4 (100%)	1/1 (100%)
MARGINS				
- Well-Defined	4/15 (27%)	-	-	-
- Ill-Defined	11/15 (73%)	5/5 (100%)	4/4 (100%)	1/1 (100%)
MASS EFFECT	9/15 (60%)	5/5 (100%)	4/4 (100%)	1/1 (100%)
INFILTRATIVE	11/15 (73%)	5/5 (100%)	4/4 (100%)	1/1 (100%)
PRE-CONTRAST				
- Homogeneous	10/15 (67%)	3/5 (60%)	4/4 (100%)	1/1 (100%)
- Heterogeneous	5/15 (33%)	2/5 (40%)	-	-
ENHANCEMENT				
- Marked	7/15 (47%)	3/5 (60%)	1/4 (25%)	-
- Moderate	8/15 (53%)	2/5 (40%)	2/4 (50%)	-
- Mild	-	-	1/4 (25%)	1/1 (100%)
- Homogeneous	2/15 (13%)	-	-	-
- Heterogeneous	13/15 (87%)	5/5 (100%)	3/4 (75%)	1/1 (100%)
- Rim	-	-	1/4 (25%)	-
MEDIAL RETROPHARYNGEAL LYMPHADENOPATHY				
- Cases	14/15 (93%)	5/5 (100%)	4/4 (100%)	1/1 (100%)
- Bilateral	8/14 (57%)	5/5 (100%)	3/4 (75%)	1/1 (100%)
- Marked	11/14 (79%)	5/5 (100%)	2/4 (50%)	-
- Moderate	1/14 (7%)	-	-	1/1 (100%)
- Mild	2/14 (14%)	-	2/4 (50%)	-
- Rounded	1/15 (7%)	4/5 (80%)	2/4 (50%)	-
- Elongated	3/14 (21%)	1/5 (20%)	2/4 (50%)	1/1 (100%)
- Homogeneous Enh.*	3/14 (21%)	-	2/4 (50%)	1/1 (100%)
- Heterogeneous Enh.	11/14 (79%)	5/5 (100%)	2/4 (50%)	-
MANDIBULAR LYMPHADENOPATHY				
- Cases	9/15 (60%)	4/5 (80%)	3/4 (75%)	1/1 (100%)
- Bilateral	3/9 (33%)	3/4 (75%)	2/3 (67%)	1/1 (100%)
- Marked	1/9 (11%)	1/4 (25%)	-	-
- Moderate	6/9 (67%)	3/4 (75%)	1/3 (33%)	-
- Mild	2/9 (22%)	-	2/3 (67%)	1/1 (100%)
- Rounded	6/9 (67%)	4/4 (100%)	1/3 (33%)	-
- Elongated	3/9 (33%)	-	2/3 (67%)	1/1 (100%)
- Homogeneous Enh.	5/9 (56%)	2/4 (50%)	3/3 (100%)	1/1 (100%)
- Heterogeneous Enh.	4/9 (44%)	2/4 (50%)	-	-
VESSELS	1/15 (6%)	-	-	-
METASTASIS				
- MRPL†	7/15 (47%)	3/5 (60%)	2/4 (50%)	-
- ML‡	0/15 (0%)	-	-	-
- Distant	0/15 (0%)	2/5 (40%)	2/4 (50%)	-
MINERALISATION	3/15 (20%)	1/5 (20%)	-	-
HYPOATTENUATING AREA	2/15 (13%)	3/5 (60%)	3/4 (75%)	-

*Enh= Enhancement.
†MRPL= Medial Retropharyngeal Lymph Nodes.
‡ML= Mandibular Lymph Nodes.

5.2 QUALITATIVE CT IMAGING FEATURES

The oropharynx was the most frequent location for carcinomas (13/15; 87%), sarcomas (4/5; 80%), melanomas (4/4; 100%) and lymphoma (1 case). Especially in the carcinoma group, the tonsillar fossa was the most represented site of affection (10/15 cases; 67%;) (Fig. 16A,C). Lesions in the laryngopharyngeal tract were seen in 8/25 cases (32%) but, in the extraskeletal osteosarcoma case (Fig. 17), the laryngopharynx was the only pharyngeal area involved. Lesions involving only the nasopharynx were reported in carcinomas, particularly an adenocarcinoma.

These tumours were mostly characterised by irregular shape (19/25; 76%), ill-defined margins (21/25; 84%) and a mixed-mass effect and an infiltrative pattern of growth, (Fig. 15C, 16A, 20A) except in carcinomas, where 4 cases (3 TSCC and 1 tonsillar carcinoma) were characterised by oval shape and well-defined margins (Fig. 16C). The lymphoma appeared as an irregular, ill-defined thickening of the oropharyngeal and laryngeal wall associated to a marked enlargement of the palatine tonsils (Fig. 20 A-B).

In the pre-contrast series, 10/15 (67%) cases of carcinomas, 3/5 (60%) of sarcomas, all melanomas (4/4; 100 %) and the lymphoma appeared homogeneous. After contrast medium administration, most of the lesions (22/25; 88%) showed a heterogeneous enhancement pattern, 2 carcinomas (13%) showed a homogeneous enhancement and 1 melanoma (25%) showed rim-enhancement pattern (Fig. 28C). Carcinomas and sarcomas had moderate (8/15; 53% and 2/5; 40%, respectively) to marked (7/15; 47% and 3/5; 60%, respectively) enhancement. In melanomas, 2/4 (50%) cases had moderate enhancement, whereas the remaining cases showed marked and mild enhancement (Fig. 19A), respectively. The lymphoma had a mild heterogeneous enhancement. Mineralisation was recognised in 3 carcinoma cases (20%): 2 within the lesions (non-TSCC) and 1 in the enlarged medial retropharyngeal lymph node (TSCC) (Fig. 16D), whereas the extraskeletal osteosarcoma, showed a widespread mineralisation of the mass and a round hypoattenuating area in the caudal part of the lesion compatible with necrotic or haemorrhagic foci (Fig. 17A).

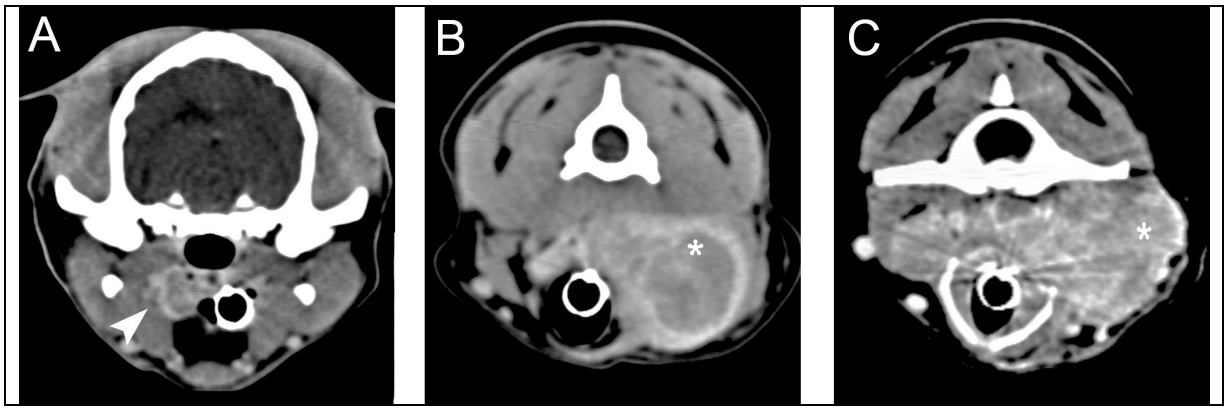

FIG. 15: Transverse soft tissue window post-contrast CT images of a male 6-year-old mongrel dog, diagnosed with tonsillar squamous cell carcinoma. A: irregular ill-defined lesion in the left tonsillar fossa (arrow head), presenting marked heterogeneous enhancing pattern. B: left medial retropharyngeal lymph node (asterisk), markedly enlarged, rounded shape, and rim-enhancing pattern. Hypoattenuating central zone represents central necrotic area. C: the same dog presented for a recurrence five months after tonsillectomy. Lesion (asterisk) appeared as a larger, irregular space-occupying lesion, with a marked heterogeneous enhancement and a more aggressive pattern of growth, extending also in the contralateral part.

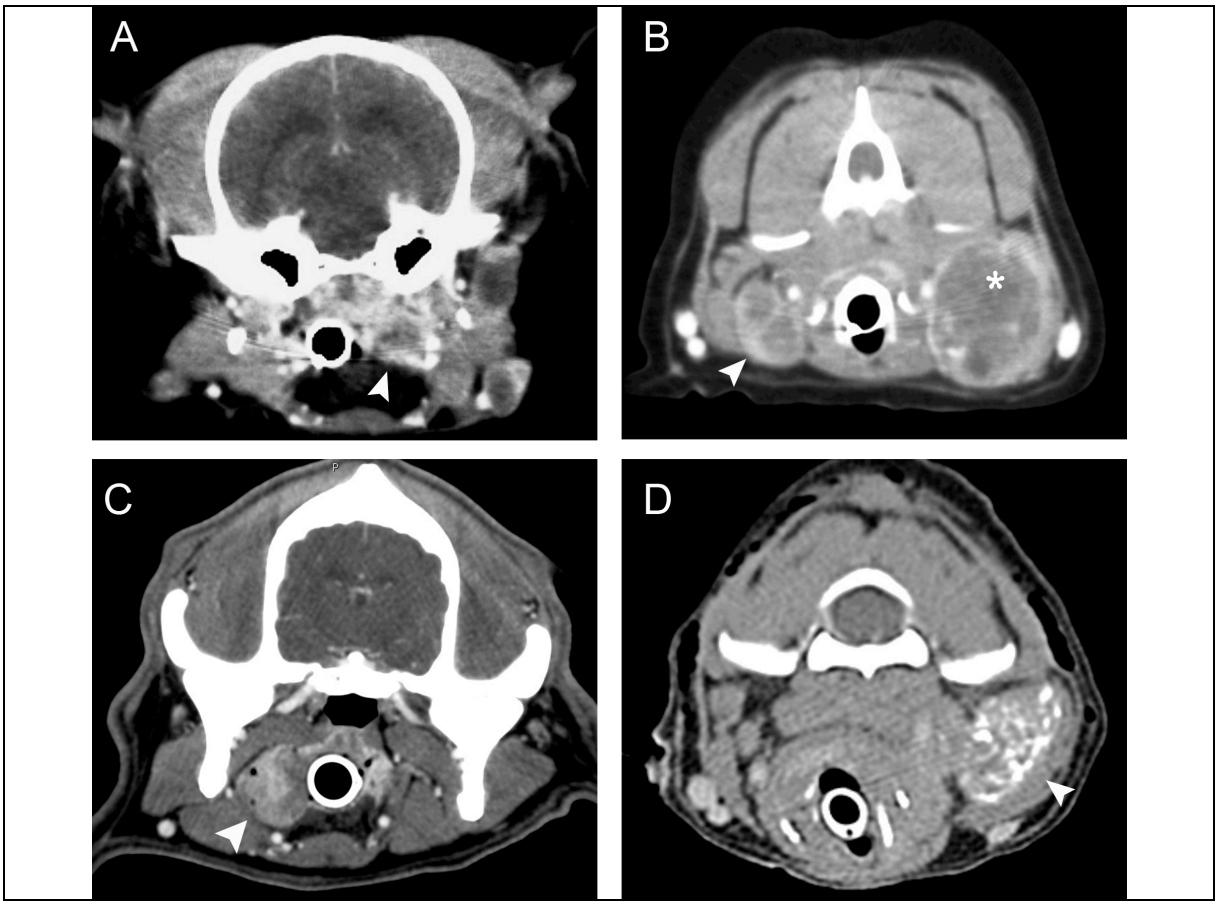

FIG. 16: Transverse soft tissue window post-contrast images of three different cases. A-B: female 10-year-old mongrel dog, diagnosed with tonsillar squamous cell carcinoma (TSCC). A: irregular ill-defined lesion (arrow head), infiltrating surrounding soft tissue and obliterating caudal nasopharynx. B: marked bilateral medial retropharyngeal lymphadenopathy. Both left (arrow head) and right (asterisk) medial retropharyngeal lymph nodes appeared markedly enlarged, rounded and with rim-enhancing pattern. Fine-needle aspiration detected metastasis in right lymph node. C: male 7-year-old Labrador Retriever, diagnosed with tonsillar squamous cell carcinoma. Contrary to Figure 2A, the lesion in the left tonsillar fossa (arrow head) has better-defined margins and shape, and heterogeneous marked enhancement. D: female 12-year-old Maltese, diagnosed with non-TSCC in the oropharyngeal and laryngopharyngeal area. Right medial retropharyngeal lymph node (arrow head) has diffuse foci of mineralisation.

Medial retropharyngeal lymph nodes enlargement, change in shape or heterogeneous contrast enhancement were present in all but one (nasopharyngeal adenocarcinoma) case (24/25; 96%), and mandibular lymphadenopathy were recorded in 68% of dogs (17/25) (Fig. 21).

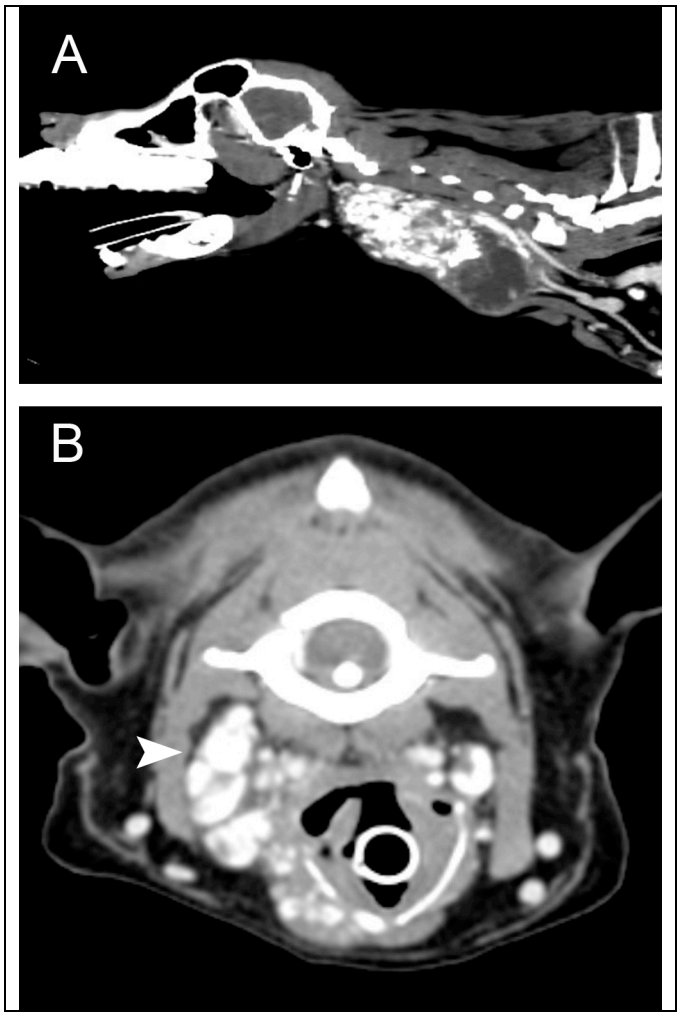

FIG. 17: Female, 8-year-old Border Collie, diagnosed with extraskeletal osteosarcoma. A: sagittal soft tissue window post-contrast multiplanar reconstruction. The lesion in the ventral region of the neck, extending from the laryngopharyngeal area to thoracic inlet, contains diffuse coalescent foci of mineralisation. A rounded hypoattenuating area of necrosis/haemorrhage is visible in the caudal part. B: transverse soft tissue window post-contrast image. Diffuse mineralisation of tissues on the left of thyroid cartilage. Also retropharyngeal lymph nodes (arrow head), are also diffusely mineralised.

In 11/14 cases of carcinomas (79%), 5/5 sarcomas (100%) and 2/4 melanomas (50%), medial retropharyngeal lymph nodes were markedly enlarged and had a rounded shape and heterogeneous enhancement (Fig. 15B; 16B; 19B). The undifferentiated sarcoma showed markedly enlarged medial retropharyngeal lymph nodes with elongated shape. The medial retropharyngeal lymph nodes were diffusely mineralised in the extraskeletal osteosarcoma case and in one TSCC case (Fig. 17B, 16D). In the remaining cases of melanoma and in the lymphoma case, medial retropharyngeal lymph nodes were, respectively, mildly enlarged (2/4; 50%) and moderately enlarged, both with elongated shape and homogeneous enhancement pattern.

Mandibular lymphadenopathy was characterised mostly by moderate enlargement (10/17; 58%; 6 carcinomas, 3 sarcomas and 1 melanoma), rounded shape (11/17; 64%) and homogeneous enhancement (11/17). Marked enlargement, round shape and heterogeneous enhancement was observed in only 2/17 (12%) cases, one TSCC and one fibrosarcoma, which showed the same alterations in the medial retropharyngeal lymph nodes. Mild enlargement, elongated shape and

homogeneous enhancement were recorded in 5/17 dogs (30%; 2 carcinomas, 2 melanomas and 1 lymphoma).

Fine needle aspirates (n=17) or biopsies (n=3) of regional lymph nodes were performed in 20/25 dogs. The lymph nodes tested were: 15 medial retropharyngeal lymph nodes (3 by histology) and 5 mandibular lymph nodes. Metastatic involvement was confirmed in medial retropharyngeal lymph nodes in 12 cases (48%; 7 carcinomas, 3 sarcomas and 2 melanomas): by cytology in 10 dogs and by histology in 2 dogs. All but one were markedly enlarged, rounded in shape and heterogeneously enhancing. In one melanoma, cytology confirmed the metastatic involvement in mildly enlarged medial retropharyngeal lymph nodes. No sampling, cytological nor histological, was performed in the lymphoma case.

Bone lysis was observed in two cases of non-TSCC (hyoid bones) and in the nasopharyngeal adenocarcinoma (presphenoid bone and cribriform plate of the ethmoid), whereas the laryngopharyngeal adenocarcinoma produced calcification on the thyroid cartilage. The lingual artery was included within the mass only in one dog (non-TSCC).

Lung nodules, recorded as potential distant metastasis, were identified in 4/25 (16%) dogs: 2 were sarcomas (extraskeletal osteosarcoma and undifferentiated sarcoma) and 2 were melanomas. None of these lesions was confirmed by cytologic or histologic examination.

5.3 QUANTITATIVE CT IMAGING FEATURES

Lesion volume was variable between and inside the groups: the mean volume (range) of carcinomas, sarcomas, and melanomas was 15.39 cm^3 (2.82 - 29.06 cm^3), 116.57 cm^3 (2.16 - 426.41 cm^3), and 16.38 cm^3 (0.6 - 43.63 cm^3), respectively. The lymphoma was 3.2 cm^3 in volume.

The largest range, in the sarcoma cases, was due to the extraskeletal osteosarcoma case, a large lesion extending from pharynx to thoracic inlet (Fig. 17A, 18).

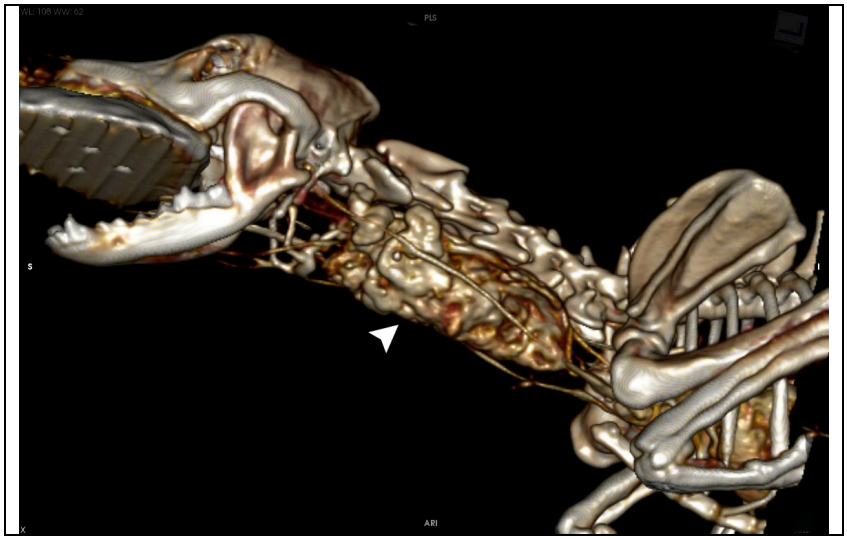

FIG. 18: Female, 8-year-old Border Collie, diagnosed with extraskeletal osteosarcoma. 3D volume rendering: The arrow head indicate the large space occupying lesion in the ventral regione of the neck. The lesion extends between larynx and thoracic inlet.

Mean pre- and post-contrast attenuation in carcinomas was 54.68 HU (±13.66) and 89.63 (±23.61), respectively. In the sarcoma group, mean HU was of 47.34 HU (±8) in the pre-contrast and 82.19 HU (±17.4) in the post-contrast series. In the melanomas, mean values of pre- and post-contrast attenuation were 50.52 HU (±14.01) and 83 HU (±31.14), respectively. The lymphoma had a mean pre- and post-contrast attenuation equal to 41.05 HU (±9.79) and 56.69 HU (±28.22), respectively.

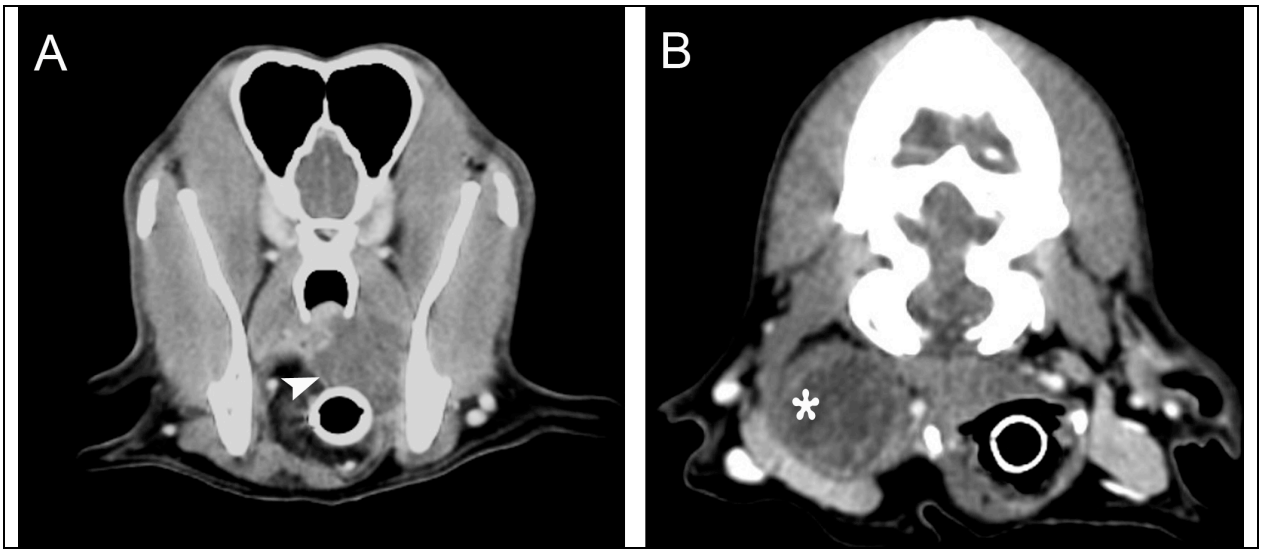

FIG. 19: Transverse soft tissue window post-contrast images of two dogs diagnosed with malignant melanoma. A: female 14-year-old Golden Retriever. The lesion (arrow head), extending from the soft palate in the oropharynx and infiltrating the pharyngeal wall, shows poor enhancement after contrast medium administration. B: male 12-year-old Cocker Spaniel, with markedly enlarged right retropharyngeal lymph node (asterisk), presenting a mild peripheral enhancing pattern with large central hypoattenuating area.

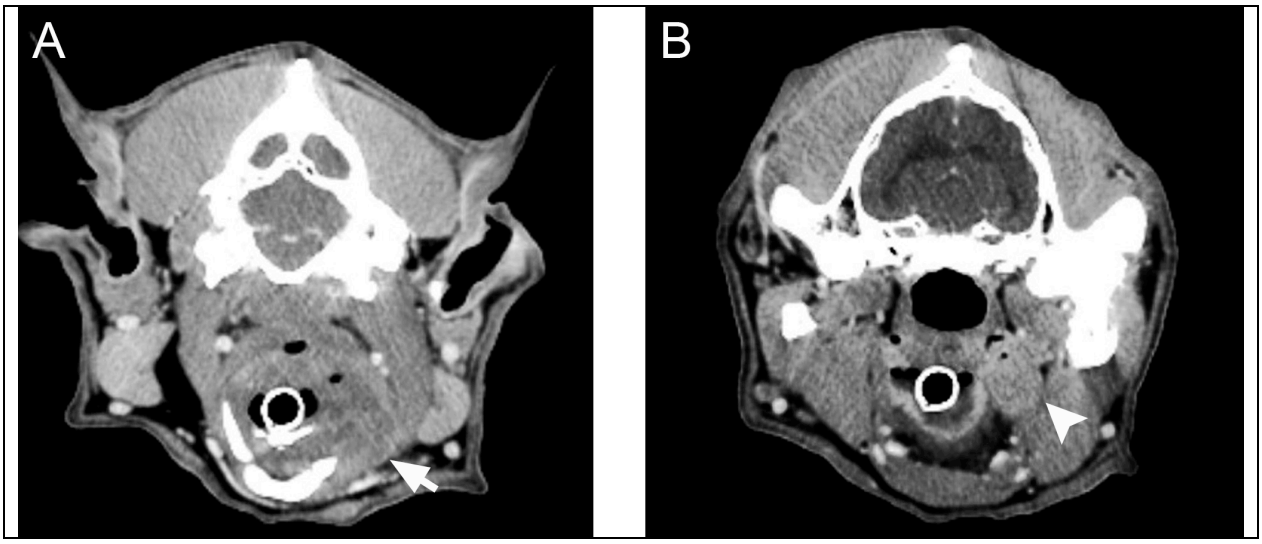

FIG. 20: Transverse soft tissue window post-contrast images of a female 11-year-old Bull Terrier, diagnosed with lymphoma. A: ill-defined thickening of right oropharyngeal and laryngopharyngeal wall, presenting mild and heterogeneous enhancement (short arrow). B: marked enlargement of omolateral palatine tonsil (arrow head).

5.4 STATISTICAL ANALYSIS

Incidence of pharyngeal malignancy in males was greater than in females for carcinomas (11/15; 73%; P=0.016), whereas a gender predisposition was not found for malignant melanoma (1/4; 25%; P=0.06) and sarcoma (3/5; 60%; P=0.756).

Statistical comparison of the qualitative CT imaging features, including shape, lesion margins, the presence of mass effect, presence of infiltration, grade and pattern of enhancement, and potential distant metastasis, as well as enlargement, shape end enhancement of lymph nodes did not differentiate the various categories of pharyngeal neoplasia from one another. All P- Values were greater than 0.05.

The quantitative CT imaging features, including mass size, pre- and post-contrast attenuation, also did not allow statistically significant differentiation of tumour type.

Medial retropharyngeal lymph nodes presenting at least one of the characteristics of enlargement, change in shape and abnormal enhancement were recorded in 96% (24/25) of cases. In 75% of these (18/24), marked enlargement, rounded shape and heterogeneous enhancement was recorded. The combination of these three subjective evaluation criteria was associated to a 75% chance of identifying nodal malignancy (P=0.006).

The following graphics (Fig. 21-27) illustrate the main findings of this study:

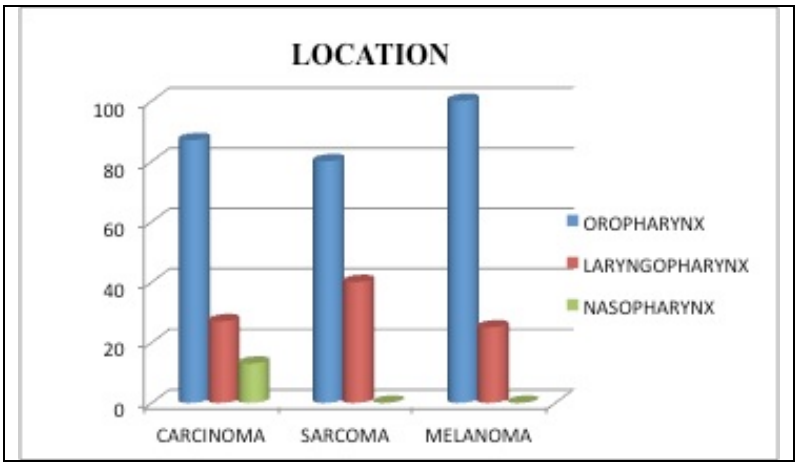

FIG. 21: the graph shows the distribution of the lesions within the different pharyngeal tracts. The oropharynx results the most frequent location, and the nasopharynx the less frequent.

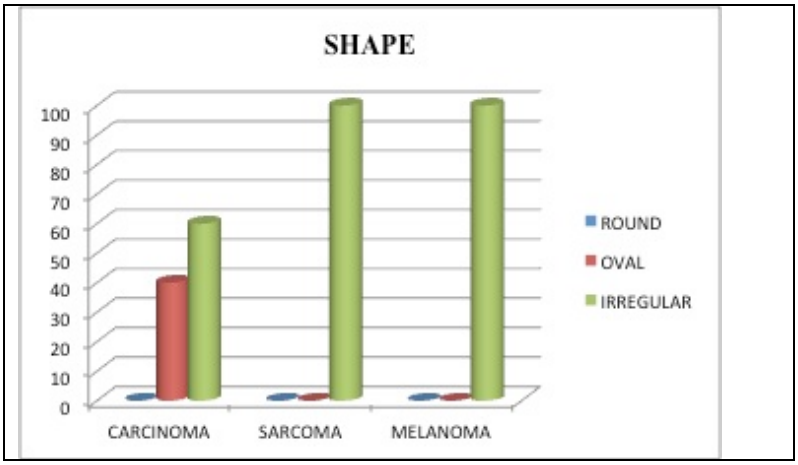

FIG. 22: the graph shows the variability of shape of the lesions. The irregular shape result the most frequent pattern.

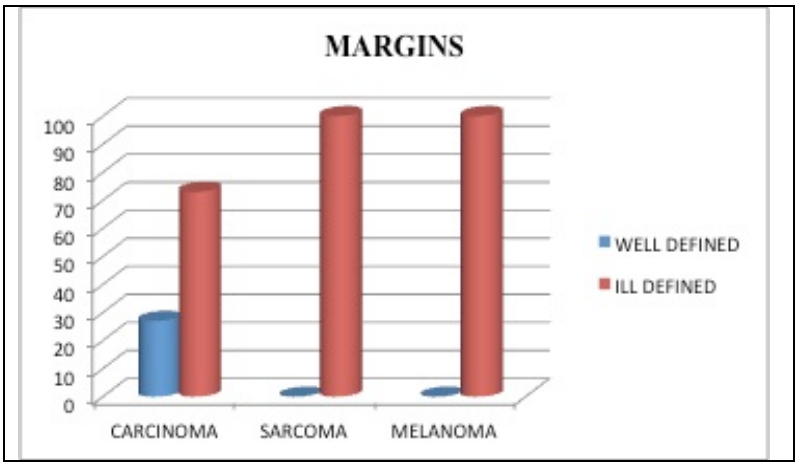

FIG. 23: as illustrated, the great majority of the lesions have ill defined margins. This feature associated with irregular shape make the surgical planning more difficult.

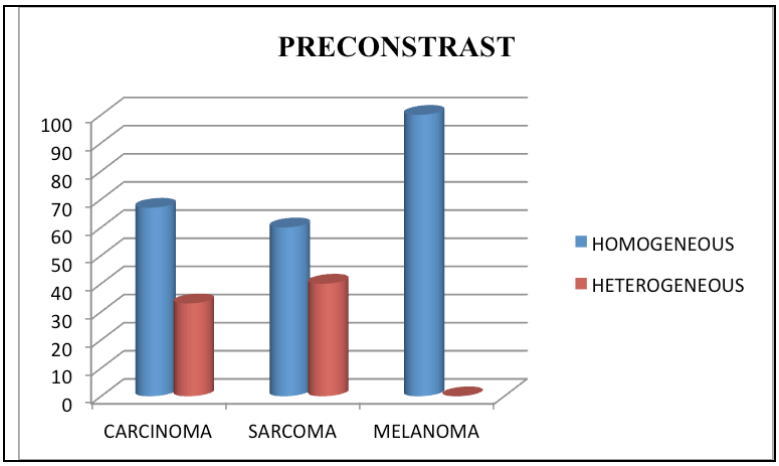

FIG. 24: Graphics shows the pattern of attenuation in the precontrast images. As illustrated, before contrast medium administration lesions are homogeneous in the majority of cases.

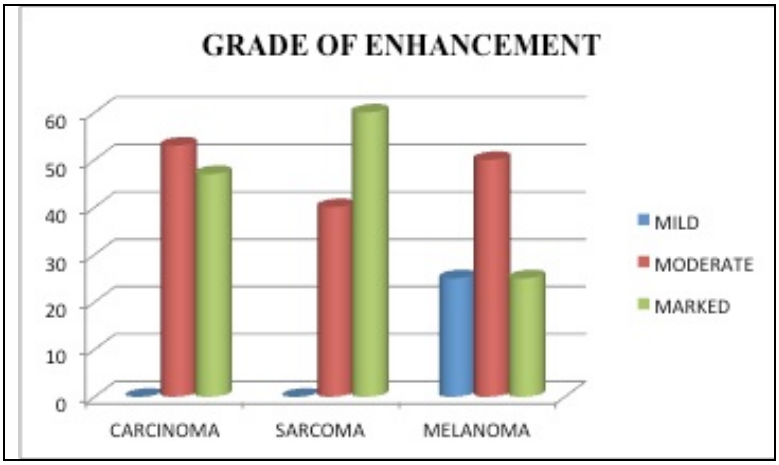

FIG. 25: Graphic shows the grade of enhancement. In the majority of case the enhancement range from moderate to marked, also in the sarcoma cases.

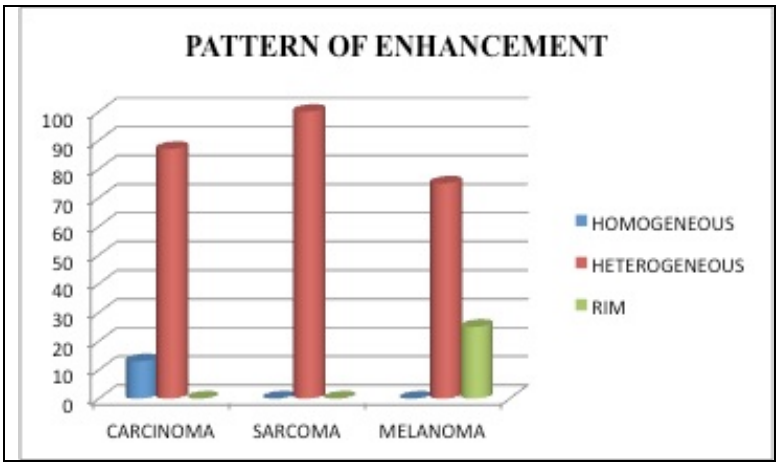

FIG. 26: Graphic shows the pattern of distribution of contrast medium. Almost all cases have heterogeneous enhancement, likely due to presence of necrotic or haemorrhagic tissue.

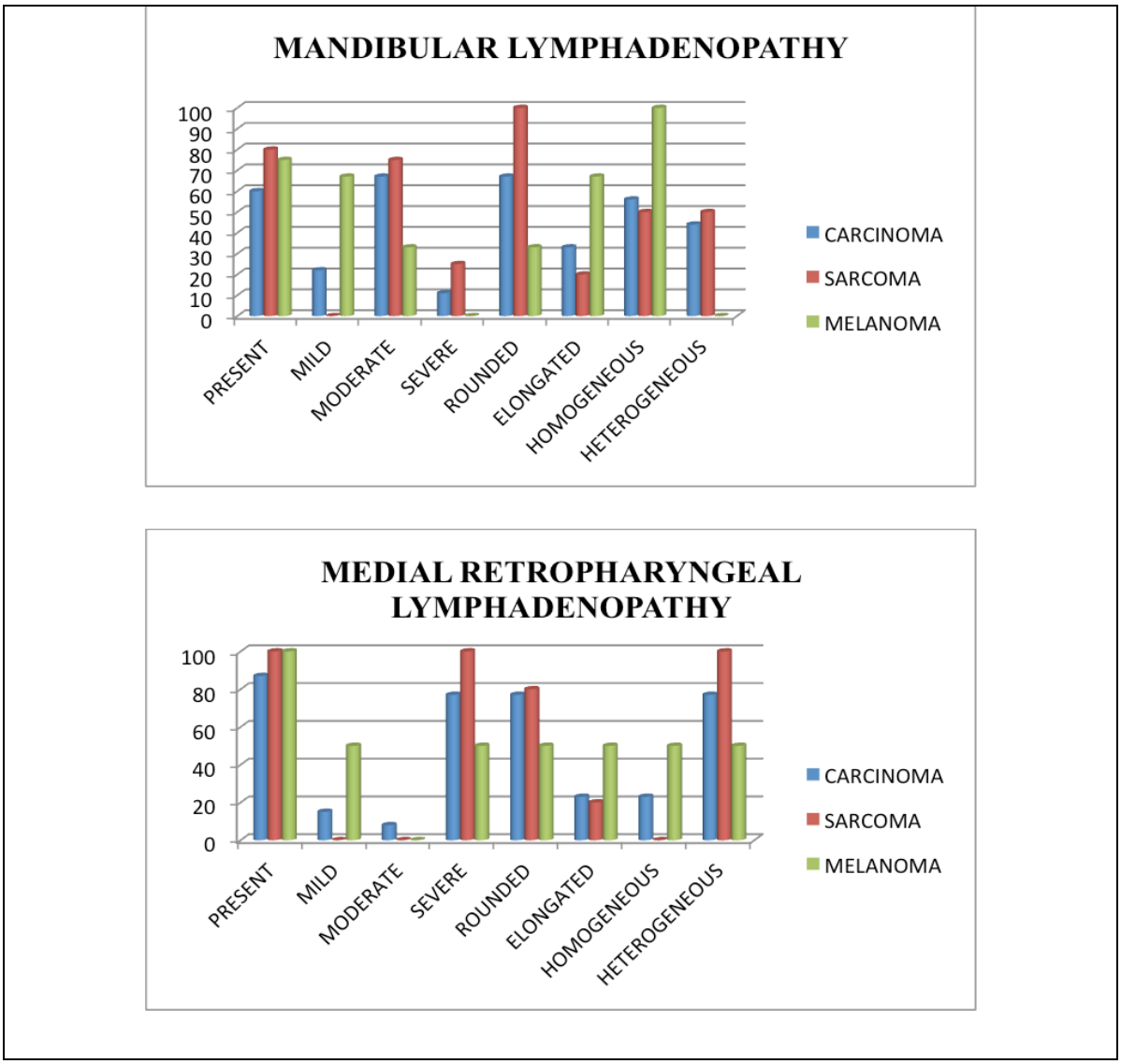

FIG. 27: These g two graphics show the different grade of involvement of the mandibular lymph nodes respect to the medial retropharyngeal lymph nodes. As highlights by the graphics the medial retropharyngeal lymph nodes are more frequently and severely involved, presenting severe enlargement, rounded shape and heterogeneous enhancement, particularly in the sarcomas cases.

CHAPTER 6

DISCUSSION

This chapter was adapted from: Carozzi F, Zotti A, Alberti M, Rossi F. Computed tomographic features of pahreyngeal neoplasia in 25 dogs. *Veterinary Radiology and Ultrasound 2015; 56 (6); 628-637.*

6.1 DISCUSSION

The pharyngeal area could be involved in different acquired or congenital diseases, ranging from foreign bodies to neoplastic disease. Neoplastic lesions of the dog share some features with respective human cancers. The study of the spontaneous neoplasia in dogs could serve as a pattern for analogous disease in human, providing a better model than chemically induced tumours, avoiding potential artifacts.[29]

The tumours arising from the pharynx in the majority of cases are expansive masses with high grade of local invasiveness and infiltrative growth pattern.[29–31,37,60,28] These features is consistent with the imaging characteristics observed in the majority of cases in this study: irregular shape and ill-defined space occupying lesions.

The oropharynx was the most common location, followed by the laryngopharynx and the nasopharynx. Our results revealed the tonsillar fossa as the most common site of pharyngeal neoplasia; such a data is consistent with the previous literature.[31,32] The lesion morphology (volume, shape, margins) and other CT features analysed and compared are not significantly different between groups as hypothesised (Fig. 28 A-D). This data differs from information reported in another study where the nasopharyngeal area was predominant. However, in that study, Billen et al. have considered also non-specific inflammatory diseases, like foreign body and abscess, or congenital conditions like nasopharyngeal stenosis and choanal atresia.[21]

Osteolysis of adjacent bone structures and infiltration of vessels were rarely detected and only in the carcinoma group. These findings, concerning oral and oropharyngeal SCC, disagree with the literature, in both human and veterinary medicine. Indeed, it is reported that these neoplasias have a propensity to spread along adjacent bone, resulting in osteolytic lesion, or through lymphatic and blood vessels.[45,46,53,61] We suppose that this discrepancy may be due to the fact that pharyngeal localisation causes early clinical signs, so patients present at an early stage, or may be because osteolysis, as reported in humans, has a late manifestation, owing to the effective barrier function of the periosteoum.[43]

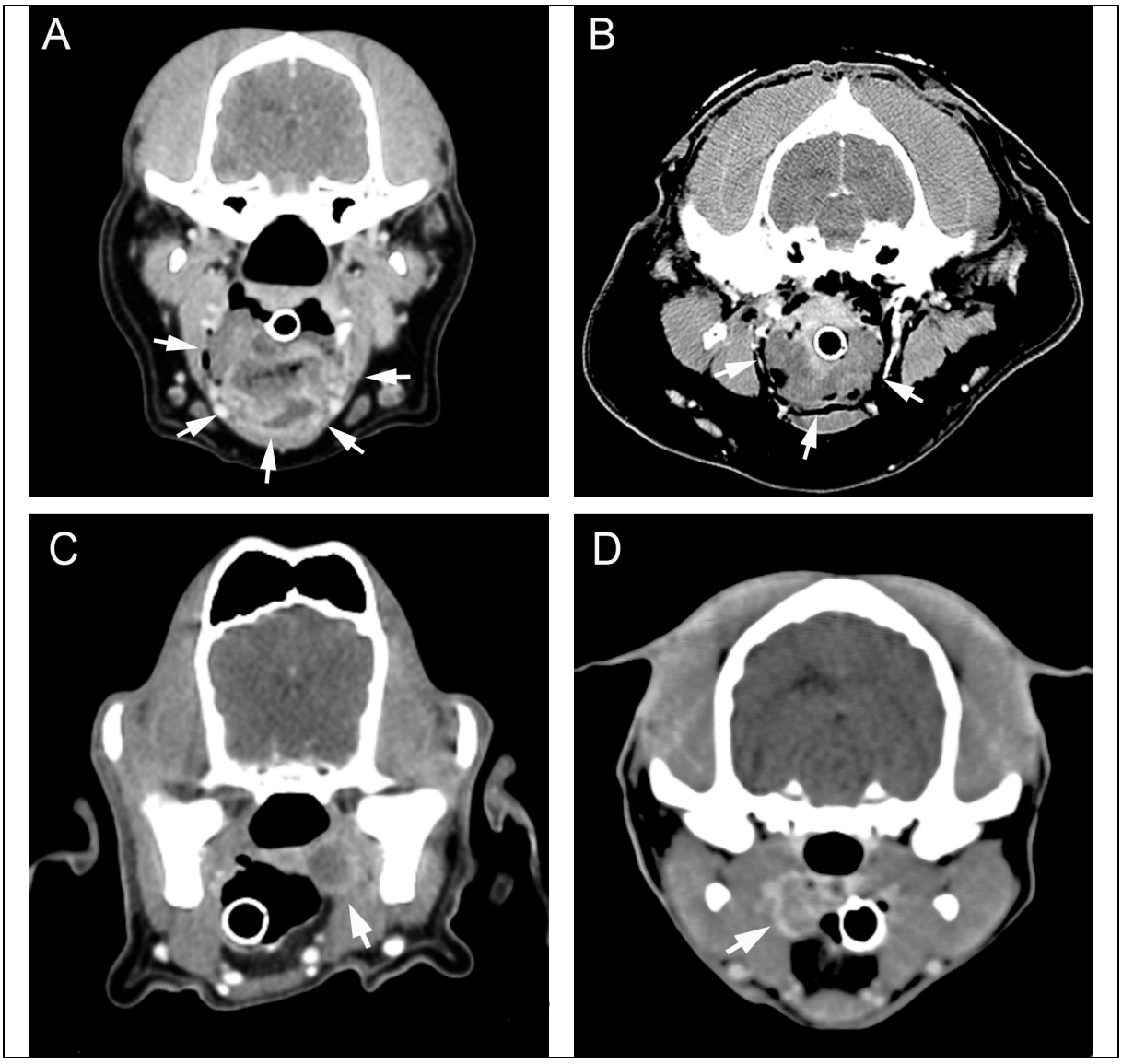

FIG. 28: Transverse soft tissue window post-contrast images of four different cases. A and B: Female 13-year-old mongrel and female 11-year-old Rottweiler, respectively. The lesions indicated by the arrows in these two different cases have similar CT features, oropharyngeal localisation, rounded shape, ill-defined margins, particularly in the ventral edge, and a similar enhancing pattern. However, case A was diagnosed as undifferentiated sarcoma, whereas B was diagnosed as malignant melanoma. C and D: Male 12-year-old Cocker Spaniel and male 6-year-old mongrel, respectively. Two lesions in the tonsillar fossa (arrow), presenting rounded shape, well-defined margins and a marked rim enhancement, which is more heterogeneous in D. They were diagnosed as malignant melanoma and tonsillar squamous cell carcinoma, respectively.

Pre- and post-contrast attenuation of the pharyngeal tumours were variable and not statistically correlated to histopathology. Before contrast medium administration, lesions were mostly homogeneous. Small foci of mineralisation were present in three SCC (2 tonsillar, 1 non-tonsillar), and more extended mineralised areas were observed in the extraskeletal osteosarcoma. On the post-contrast series, almost all lesions showed a moderate-to-marked heterogeneously enhancing pattern,

including the sarcomas. Based on these data, post-contrast venous vascularisation characteristics are not a useful criterion in predicting histopathology before biopsy. However other studies, performing dynamic CT studies[25] or colour/power Doppler[62,63] of tumours vascularisation, report an higher vascularity in carcinoma and lower vascularity in soft tissue sarcoma. The moderate-to-marked enhancement also in the sarcoma cases could be explained, in our opinion, by the strong enhancement of the surrounding soft tissues of the pharyngeal region, indicating a high vascularity.[28]

Tumour volume was not statistically significant between the different tumour types. The lowest volume range (0.6 cm^3) detected in a melanoma suggests that lesion, particularly in the early stage, could be overlooked, due to silhouetting with adjacent structures. Thus, to avoid this, the open mouth position should be chosen for more accurate pharynx examination, as recommended in a previous study.[17] The higher volume range in the sarcoma group was due to the presence of a single very large mass (extraskeletal osteosarcoma), extending from pharynx to thoracic inlet. Unusual imaging features characterised this neoplasia. Extraskeletal osteosarcoma is a rare, osteoid-producing neoplasm and most commonly affects visceral sites, skin or subcutaneous tissue, or mammary glands.[64,65] CT scans showed a large soft tissue mass with extensive calcification/ossification, also involving medial retropharyngeal lymph nodes, with a large hypoattenuating area compatible with necrotic or haemorrhagic foci. These characteristics are almost identical to CT features of extraskeletal osteosarcoma in humans.[66]

In an oncologic patient, the role of imaging is not limited to characterisation of the local disease but includes a complete staging.[67] Metastatic lymph node involvement, within our study population, was slightly higher if compared with the literature.[68] Metastatic risk in SCC has been reported as site-dependent, based on primary location: lower for the rostral oral cavity and higher for the caudal tongue and tonsils.[30–32,37,38] In TSCC, there is a high percentage of tumours with bilateral incidence,[30,37,60] and we also recorded one case with bilateral affection of tonsils, associated to bilateral metastatic spread to medial retropharyngeal lymph nodes. However TSCC is considered

systemic at diagnosis in over 90% of dogs and cats.[30] Furthermore the medial retropharyngeal lymph nodes drain the lymph directly from the palatine tonsil,[27] therefore, they are likely the first site of potential nodal metastatic spread of tonsillar neoplasia.

Sarcomas, particularly fibrosarcoma, are characterised by extensive local infiltration and slow growth, whereas metastasis to regional lymph nodes and distant metastasis are uncommon.[29–31,37] However, some histotypes, such as histiocytic sarcoma[69,70] and extraskeletal osteosarcoma, have an aggressive systemic behaviour with a high metastatic rate.[64,65] Marked medial retropharyngeal lymphadenomegaly was present in all sarcoma cases, and confirmed as metastatic in all sampled nodes (3/5). All these lymph nodes presented heterogeneous enhancement with central hypoattenuating area, and rounded shape.

Malignant melanoma is characterised by rapid growth, early local invasion, frequent recurrence and early metastasis to regional nodes and lungs.[30,34,36,37] Microscopic metastatic involvement in normal-sized mandibular lymph nodes was reported in 40% of the dogs in a previous study.[44] Therefore, bilateral sampling of lymph nodes, even if not enlarged, is mandatory. Being a site of metastases of melanoma, also the tonsils should be included in the staging.

Canine lymphomas present usually as multi-centric disease, and high grade.[29] The single case in our study population presented regional and abdominal lymphadenopathy. Lymphoma can affect the tonsils but is usually accompanied by generalised lymphadenopathy and is often bilateral.[30]

One of the most important findings of this thesis was that medial retropharyngeal lymph nodes were, based on CT abnormalities, more frequently involved than mandibular lymph nodes. Mandibular lymph nodes are more commonly evaluated in routine clinical staging, probably since they are easier to access with palpation due to their superficial location. Retropharyngeal lymph nodes are located more deeply and lymphadenomegaly is difficult to identify clinically, even if pronounced. However, they are in closer relationship with the pharyngeal structures and firmly connected by a dense network of lymphatic and blood vessels originating from the deep parts of the head.[24] In this study medial retropharyngeal lymph nodes showed marked enlargement, rounded shape and

heterogeneous enhancement in the majority of cases. This finding is consistent with another study reporting that the presence of metastases from oral and maxillofacial neoplasia may be overlooked if only the mandibular lymphocentrum is evaluated.[68] In the human literature, CT imaging criteria for identification of a metastatic lymph node include the following parameters: maximum diameter > 10-15 mm, rounded shape, central area of decreased attenuation of the node (necrosis), nodal extension beyond its capsular margin, rim enhancement with contrast, or grouping of three or more lymph nodes in an area of high-risk nodal drainage.[51,54–56] Nodal enlargement and central hypoattenuation area were considered criteria highly suggestive of metastasis.[51,54] An area of decreased attenuation in a lymph node could be representative of tumour cells as well as necrotic tissue or both.[54] However, lipid metaplasia or an abscessed node may resemble necrosis secondary to metastasis on CT.[54] Furthermore, a recent veterinary study[57] reported that nodal enlargement and heterogeneous enhancement could be helpful to differentiating nodal metastatic involvement. The criteria evaluated in our study - marked enlargement, rounded shape and heterogeneous enhancement - associated with a 75% chance of nodal metastatic spread - are in agreement with these data. In humans, identification of metastatic cervical lymphadenopathy is recognised as the most important prognostic indicator in patients with SCC.[52,71] The presence of ipsilateral or bilateral metastatic lymphadenopathy significantly reduces patient survival time.[52] Therefore, an effort must also be made in veterinary medicine to sample all regional lymph nodes.

The limitations of this present study are the small number of cases and the high variability between and within groups. The single lymphoma case did not allow comparison with other tumour groups and was excluded from statistical analysis. Due to the retrospective design of this study, the enhancement pattern of the lesions has been studied only in the venous phase. Furthermore, owing to design of this study a few of the cytology or histology reports were unavailable; hence statistical analysis of this parameter was based on 80% of the data (20/25 cases).

6.2 CONCLUSION

Computed tomography plays a crucial role in characterizing location and extension of the pharyngeal lesion, lymph nodes involvement and presence of distant metastatic spread in dogs with pharyngeal neoplasia. In spite of its high sensitivity, the specificity of CT imaging is low. In this study the CT findings were overlapping in the different groups of pharyngeal neoplasia, and therefore histotype could not be predicted. Biopsy is always required for a final diagnosis. However, as highlighted in this study, CT is fundamental to verify presence of nodal metastasis and/or locating lymph nodes to sample, particularly those not easily achievable during clinical examination. Furthermore to perform a complete and accurate staging of the patient, in the authors' opinion, the medial retropharyngeal lymph nodes analysis should be included in staging of pharyngeal neoplasia, It is possible that further studies involving larger sample of dogs or based on different CT technique, for example dynamic protocols, will be useful to better characterize the CT findings of pharyngeal neoplasia. Moreover, our preliminary results about association between imaging features and metastatic lymph nodes should be confirmed by additional prospective studies.

BIBLIOGRAPHY

1. Burk RL. Computed tomographic anatomy of the canine nasal passages. *Vet Radiol Ultrasound*. 1992;33(3):170-176.

2. De Rycke LM, Saunders JH, Gielen IM, van Bree HJ, Simoens PJ. Magnetic resonance imaging, computed tomography, and cross-sectional views of the anatomy of normal nasal cavities and paranasal sinuses in mesaticephalic dogs. *Am J Vet Res*. 2003;64(9):1093-1098.

3. Burk RL. Computed Tomographic Imaging of Nasal Disease in 100 Dogs. *Vet Radiol Ultrasound*. 1992;33(3):177-180.

4. Miles MS, Dhaliwal RS, Moore MP, Reed AL. Association of magnetic resonance imaging findings and histologic diagnosis in dogs with nasal disease: 78 cases (2001-2004). *J Am Vet Med Assoc*. 2008;232(12):1844-1849.

5. Saunders JH, Zonderland JL, Clercx C, et al. Computed tomographic findings in 35 dogs with nasal aspergillosis. *Vet Radiol Ultrasound*. 2002;43(1):5-9.

6. Avner a., Dobson JM, Sales JI, Herrtage ME. Retrospective review of 50 canine nasal tumours evaluated by low-field magnetic resonance imaging. *J Small Anim Pract*. 2008;49(5):233-239.

7. Petite AFB, Dennis R. Comparison of radiography and magnetic resonance imaging for evaluating the extent of nasal neoplasia in dogs. *J Small Anim Pract*. 2006;47(9):529-536.

8. Taeymans O, Schwarz T, Duchateau L, et al. Computed tomographic features of the normal canine thyroid gland. *Vet Radiol Ultrasound*. 2008;49(1):13-19.

9. Taeymans O, Dennis R, Saunders JH. Magnetic resonance imaging of the normal canine thyroid gland. *Vet Radiol Ultrasound*. 2008;49(3):238-242.

10. Taeymans O, Penninck DG, Peters RM. Comparison between clinical, ultrasound, ct, mri, and pathology findings in dogs presented for suspected thyroid carcinoma. *Vet Radiol Ultrasound*. 2013;54(1):61-70.

11. Deitz K, Gilmour L, Wilke V, Riedesel E. Computed tomographic appearance of canine thyroid tumours. *J Small Anim Pract*. 2014;55(6):323-329.

12. Rossi F, Caleri E, Bacci B, et al. Computed tomographic features of basihyoid ectopic thyroid carcinoma in dogs. *Vet Radiol Ultrasound*. 2013;54(6):575-581.

13. Taeymans O, Peremans K, Saunders JH. Thyroid imaging in the dog: current status and future directions. *J Vet Intern Med*. 2007;21(4):673-684.

14. Mai W, Seiler GS, Lindl-bylicki BJ, Zwingenberger AL. Ct and Mri Features of Carotid Body Paragangliomas in 16 Dogs. *Vet Radiol Ultrasound*. 2015;56(4):374-383.

15. Fife W, Mattoon J, Drost WT, Groppe D, Wellman M. Imaging features of a presumed carotid body tumor in a dog. *Vet Radiol Ultrasound*. 2003;44(3):322-325.

16. Kromhout K, Gielen I. Magnetic resonance and computed tomography imaging of a carotid body tumor in a dog. *Acta Vet Scand*. 2012;(Figure 1):2-7.

17. Laurenson MP, Zwingenberger AL, Cissell DD, et al. Computed tomography of the pharynx in a closed vs. open mouth position. *Vet Radiol Ultrasound*. 2011;52(4):357-361.

18. Berent AC, Kinns J, Weisse C. Balloon dilatation of nasopharyngeal stenosis in a dog. *J Am Vet Med Assoc*. 2006;229(3):385-388.

19. Nicholson I, Halfacree Z, Whatmough C, Mantis P, Baines S. Computed tomography as an aid to management of chronic oropharyngeal stick injury in the dog. *J Small Anim Pract*. 2008;49(September):451-457.

20. Clements DN, Thompson H, Johnson VS, Clarke SP, Doust RT. Diagnosis and surgical treatment of a nasopharyngeal cyst in a dog. *J Small Anim Pract*. 2006;47(11):674-677.

21. Billen F, Day M, Clercx C. Diagnosis of pharyngeal disorders in dogs: a retrospective study of 67 cases. *J Small Anim Pract*. 2006;47(March):122-129.

22. Evans H, Lahunta A De. Th Digestive Apparatus and abdomen. In: Evans H, De Lahunta A. Miller's Anatomy of the Dog. In: W.B. Saunders Company, ed. 4th ed. Philadelphia; 2013:303-304.

23. Alexander K. The pharynx, larynx, and trachea. In: Thrall DE. Textbook of Veterinary Diagnostic Radiology. In: Saunders E, ed. 6th ed. St. Louis; 2013:489-499.

24. Bezuidenhout A. *The Lymphatic System. In: Evans H, De Lahunta A. Miller's Anatomy of the Dog.* 4th ed. (W. B. Saunders Company, ed.). Philadelphia; 2013.

25. Kneissl S, Probst A. Comparison of computed tomographic images of normal cranial and upper cervical lymph nodes with corresponding E12 plastinated-embedded sections in the dog. *Vet J*. 2007;174(2):435-438.

26. Taeymans O. Lymph nodes of head and neck. In: Schwarz T and Saunders J. Veterinary Computed Tomography pp:171-175. Oxford Wiley-Blackwell 2011 1st ed. In: Wiley-Blackwell, ed. 1st ed. Oxford; 2011:171-174.

27. Belz GT, Heath TJ. Lymph pathways of the medial retropharyngeal lymph node in dogs. *J Anat*. 1995;186 (Pt 3:517-526..

28. Taeymans O, Schwarz T. Pharynx, Larynx and Thyroid Gland. In: Schwarz T and Saunders J. Veterinary computed tomography. In: Wiley-Blackwell, ed. 1st ed. Oxford; 2011:175-185.

29. MacEwen EG. Spontaneous tumors in dogs and cats: models for the study of cancer biology

and treatment. *Cancer metastasis Rev*. 1990;9(2):125-136.

30. Liptak J, Withrow S. *Cancer of the Gastrointestinal Tract. In: Withrow SJ, Vail DM, Page RL. Withrow and MacEwen's Small Animal Clinical Oncology*. 5th ed. (Saunders Elsevier, ed.). St. Louis, MO; 2013.

31. Todoroff R, Brodey R. Oral and pharyngeal neoplasia in the dog: a retrospective survey of 361 cases. *J Am Vet Med Assoc*. 1979;175(6):567-571.

32. Clarke B, Mannion P, White R. Rib metastases from a non-tonsillar squamous cell carcinoma in a dog. *J Small Anim Pract*. 2011;52(March):163-167.

33. Gor DM, Langer JE, Loevner L a. Imaging of cervical lymph nodes in head and neck cancer: The basics. *Radiol Clin North Am*. 2006;44:101-110.

34. Ramos-Vara JA, Beissenherz ME, Miller MA, et al. Retrospective Study of 338 Canine Oral Melanomas with Clinical, Histologic, and Immunohistochemical Review of 129 Cases. *Vet Pathol*. 2000;37(6):597-608.

35. Cohen D, Brodey R, Chen S. Epidemiologic aspects of oral and pahryngeal neoplasms of the dog. *Am J Vet Res*. 1964;25(109):1776-1779.

36. Bergman PJ. Canine oral melanoma. *Clin Tech Small Anim Pract*. 2007;22(2):55-60.

37. Brodey R. The biological behaviour of canine oral and pharyngeal neoplasms. *J Small Anim Pract*. 1970;11(1):45-54.

38. Fulton AJ, Nemec A, Murphy BG, Kass PH, Verstraete FJM. Risk factors associated with survival in dogs with nontonsillar oral squamous cell carcinoma 31 cases (1990-2010). *J Am Vet Med Assoc*. 2013;243(5):696-702.

39. Liggett AD, Weiss R, Thomas KL. Canine Laryngopharyngeal Rhabdomyoma Resembling

an Oncocytoma: Light Microscopic, Ultrastructural and Comparative Studies. *Vet Pathol*. 1985;22(6):526-532.

40. Barnhart K, Lewis B. Laryngopharyngeal mass in a dog with upper airway obstruction. *Vet Clin Pathol*. 2000;29(2):47-50.

41. Confer AW, DePaoli A. Primary neoplasms of the nasal cavity, paranasal sinuses and nasopharynx in the dog. *Vet Pathol*. 1978;15(1):18-30.

42. Tart RP, Kotzur IM, Mancuso a a, Glantz MS, Mukherji SK. CT and MR imaging of the buccal space and buccal space masses. *Radiographics*. 1995;15:531-550.

43. Sigal R, Zagdanski A, Schwaab G. CT and MR imaging of squamous cell carcinoma of the tongue and floor of the mouth. *Radiographics*. 1996;16(4):787-810.

44. Williams L, Packer R. Association between lymph node size and metastasis in dogs with oral malignant melanoma: 100 cases (1987-2001). *J Am Vet Med Assoc*. 2003;222(9):1234-1236.

45. Gendler A, Lewis J, Reetz JA, Schwarz T. Computed tomographic features of oral squamous cell carcinoma in cats: 18 cases (2002–2008). *J Am Vet Med Assoc*. 2010;236(3):319-325.

46. Soukup J, Snyder C, Simmons B, Pinkerton M, Chun R. Clinical, Histologic, and Computed Tomographic Features of Oral Papillary Squamous Cell Carcinoma in Dogs: 9 cases (2008-2011). *J Vet Dent*. 2013;30(1):18-24.

47. White R. Clinical staging for oropharyngeal malignancies in the dog. *J Small Anim Pract*. 1985;26(10):581-594.

48. Patel SG, Shah JP. TNM staging of cancers of the head and neck: striving for uniformity among diversity. *CA Cancer J Clin*. 2005;55(4):242-258.

49. Owen L. TNM Classification of tumours in domestic animals. *World Heal Organ*. 1980:46-

47.

50. Kusewitt D, Rush L. *Neoplasia and Tumor Biology. In: McGavin MD, Zachary JF. Pathologic Basis of Veterinary Disease.* 4th ed. (Mosby, ed.). St. Louis; 2007.

51. Prehn RB, Pasic TR, Harari PM, Brown WD, Ford CN. Influence of computed tomography on pretherapeutic tumor staging in head and neck cancer patients. *Otolaryngol Head Neck Surg*. 1998;119(6):628-633.

52. Madison MT, Remley KB, Latchaw RE, Mitchell SL. Radiologic diagnosis and staging of head and neck squamous cell carcinoma. *Radiol Clin North Am*. 1994;32(1):163-181.

53. Trotta BM, Pease CS, Rasamny JJ, Raghavan P, Mukherjee S. Oral Cavity and Oropharyngeal Squamous Cell Cancer: Key Imaging Findings for Staging and Treatment Planning. *Radiographics*. 2011;31(2):339-354.

54. Som P. Detection of Metastasis in Cervical Lymph Nodes: CT and MR Criteria and Diferential Diagnosis. *Am J Roentgenol*. 1992;158(May):961-969.

55. Kau R, Alexiou C, Stimmer H, Arnold W. Diagnostic Procedures for Detection of Lymph Node Metastases in Cancer of the Larynx. *ORL-head neck Surg*. 2000;62:199-203.

56. Anzai Y, Brunberg JA, Lufkin RB. Imaging of nodal metastases in the head and neck. *J Magn Reson Imaging*. 1991;7(5):774-783.

57. Ballegeer E a., Adams WM, Dubielzig RR, Paoloni MC, Klauer JM, Keuler NS. Computed Tomography Characteristics of Canine Tracheobronchial Lymph Node Metastasis. *Vet Radiol Ultrasound*. 2010;51(4):397-403.

58. Johnson PJ, Elders R, Pey P, Dennis R. Clinical and Magnetic Resonance Imaging Features of Inflammatory Versus Neoplastic Medial Retropharyngeal Lymph Node Mass Lesions in Dogs and Cats. *Vet Radiol Ultrasound*. 2015;0(0):1-9.

59. Randall D, Lysack J, Hudon M, et al. Diagnostic utility of central node necrosis in predicting extracapsular spread among oral cavity squamous cell carcinoma. *Head Neck*. 2015;37:92-96.

60. Mas A, Blackwood L, Cripps P, et al. Canine tonsillar squamous cell carcinoma: a multi-centre retrospective review of 44 clinical cases. *J Small Anim Pract*. 2011;52(7):359-364.

61. Nemec A, Murphy B, Kass PH, Verstraete FJM. Histological subtypes of oral non-tonsillar squamous cell carcinoma in dogs. *J Comp Pathol*. 2012;147(2-3):111-120.

62. Nitzl D, Ohlerth S, Mueller-Schwandt F, Angst A, Roos M, Kaser-Hotz B. Dynamic Computed Tomography To Measure Tissue Perfusion In Spontaneous Canine Tumors. *Vet Radiol Ultrasound*. 2009;50(4):347-352.

63. Schärz M, Ohlerth S, Achermann R, et al. Evaluation of quantified contrast-enhanced color and power Doppler ultrasonography for the assessment of vascularity and perfusion of naturally occurring tumors in dogs. *Am J Vet Res*. 2005;66(1):21-29.

64. Ehrhart N, Ryan S, Fan T. Tumors of the Skeletal System. In: Withrow SJ, Vail DM, Page RL. Withrow and MacEwen's Small Animal Oncology. In: Saunders Elsevier, ed. St. Louis, MO; 2013:463-503.

65. Duffy D, Selmic LE, Kendall a. R, Powers BE. Outcome following treatment of soft tissue and visceral extraskeletal osteosarcoma in 33 dogs: 2008-2013. *Vet Comp Oncol*. 2015:n/a - n/a.

66. Hoch M, Ali S, Agrawal S, Wang C, Khurana JS. Extraskeletal osteosarcoma: a case report and review of the literature. *J Radiol Case Rep*. 2013;7(7):15-23.

67. LeBlanc AK, Daniel GB. Advanced imaging for veterinary cancer patients. *Vet Clin North Am Small Anim Pract*. 2007;37(6):1059-1077; v - i.

68. Herring ES, Smith M, Robertson J. Lymph node staging of oral and maxillofacial neoplasms

in 31 dogs and cats. *J Vet Dent*. 2002;19:122-126.

69. Affolter VK, Moore PF. Localized and Disseminated Histiocytic Sarcoma of Dendritic Cell Origin in Dogs. *Vet Pathol*. 2002;39(1):74-83.

70. Fulmer A, Mauldin G. Canine histiocytic neoplasia: an overview. *Can Vet J*. 2007;48(10):1041-1043, 1046-1050.

71. Trotta B, Pease C, Rasamny J. Oral cavity and oropharyngeal squamous cell cancer: key imaging findings for staging and treatment planning. *Radiographics*. 2011;31:339-354.

Scientific articles published on peer-reviewed journal during the PhD Course:

- **Carozzi G**, Zotti A, Alberti M, Rossi F. Computed tomographic features of pharyngeal neoplasia in 25 dogs. Veterinary Radiology and Ultrasound; 56 (6), 2015: 628-637.
- De Strobel F, **Carozzi G**, Arboit F, Calò P, Mandara MT, Zotti A, Bernardini M. Analisi delle caratteristiche in risonanza magnetica di 12casi di patologie intracraniche non neoplastiche con diagnosi istologica nel cane e confronto con la letteratura. VETERINARIA; 27 (2), 2013: 7-22.
- **Carozzi G**, de Strobel F, Bevilacqua G, Arboit F, Mandara MT, Zotti A, Bernardini M. Analisi delle caratteristiche in risonanza magnetica di 35 neoplasie intracraniche del cane confermate istologicamente e confronto con la letteratura. VETERINARIA; 27 (1), 2013: 9-27.

Articoli scientifici su rivista pubblicati durante il Corso di dottorato:

- **Carozzi G**, Zotti A, Alberti M, Rossi F. Computed tomographic features of pharyngeal neoplasia in 25 dogs. Veterinary Radiology and Ultrasound; 56 (6), 2015: 628-637.
- De Strobel F, **Carozzi G**, Arboit F, Calò P, Mandara MT, Zotti A, Bernardini M. Analisi delle caratteristiche in risonanza magnetica di 12casi di patologie intracraniche non neoplastiche con diagnosi istologica nel cane e confronto con la letteratura. VETERINARIA; 27 (2), 2013: 7-22.
- **Carozzi G**, de Strobel F, Bevilacqua G, Arboit F, Mandara MT, Zotti A, Bernardini M. Analisi delle caratteristiche in risonanza magnetica di 35 neoplasie intracraniche del cane confermate istologicamente e confronto con la letteratura. VETERINARIA; 27 (1), 2013: 9-27.